INFLUENCE OF INHIBITOR ON CORROSION BEHAVIOUR OF AL-MG ALLOY

MUHAMAD NUR IRFAN BIN MOHD ADLY

RESEARCH PROJECT SUBMITTED IN PARTIAL FULFILMENT OF THE REQUIREMENTS FOR THE DEGREE OF MASTER OF MECHANICAL ENGINEERING

FACULTY OF ENGINEERING
UNIVERSITY OF MALAYA
KUALA LUMPUR

2021

UNIVERSITY OF MALAYA
ORIGINAL LITERARY WORK DECLARATION

Name of Candidate: Muhamad Nur Irfan Bin Mohd Adly

Matric No: S2001090

Name of Degree: Master of Mechanical Engineering

Title of Research Report ("this Work"): Influence of Inhibitor on Corrosion Behaviour of AL-MG Alloy

Field of Study: Corrosion

I do solemnly and sincerely declare that:

(1) I am the sole author/writer of this Work;
(2) This Work is original;
(3) Any use of any work in which copyright exists was done by way of fair dealing and for permitted purposes and any excerpt or extract from, or reference to or reproduction of any copyright work has been disclosed expressly and sufficiently and the title of the Work and its authorship have been acknowledged in this Work;
(4) I do not have any actual knowledge nor do I ought reasonably to know that the making of this work constitutes an infringement of any copyright work;
(5) I hereby assign all and every rights in the copyright to this Work to the University of Malaya ("UM"), who henceforth shall be owner of the copyright in this Work and that any reproduction or use in any form or by any means whatsoever is prohibited without the written consent of UM having been first had and obtained;
(6) I am fully aware that if in the course of making this Work I have infringed any copyright whether intentionally or otherwise, I may be subject to legal action or any other action as may be determined by UM.

Candidate's Signature Date: 01/09/2021

Subscribed and solemnly declared before,

Witness's Signature Date: 01/09/2021

Name: Dr. Edzrol Niza

Designation: Senior Lecturer

INFLUENCE OF INHIBITOR ON CORROSION BEHAVIOUR OF AL-MG ALLOY

ABSTRACT

From pure aluminium to a series of aluminium alloy, the evolution of the steel led by a continuous demand for a superior and more efficient steel. Since then, aluminium alloy have been employed in numerous engineering applications such as engine parts, marine applications, and other applications demands the large volumes of aluminium alloys. However, Al-Mg are exposed to continuous attacks from corrosion, thus usage of corrosion inhibitors is necessary to enhance Al-Mg corrosion resistance. The aim of this research is to study the previous literature journal on the effect of inorganic inhibitor on Al-Mg in corrosive media and surface morphology of Al-Mg with or without inorganic inhibitors from.

Electrochemical corrosion testing was performed on Al-Mg alloy with various type corrosive media and inorganic inhibitor. The corrosion mechanism with or without inhibited on Al-Mg was observed by potentiodynamic polarization study. Scanning electron microscopy (SEM) and energy dispersive X-ray spectroscopy (EDS) were used to investigate the surface microstructure morphology. The result from the reviewed journal shows that the Al-Mg was seriously corroded under acidic corrosive media due to the aggressive ion. Addition of inorganic inhibitors such as chromates, molybdates, phosphates and nitrates proved to reduce the rate of corrosion of the Al-Mg alloy. The result from the literature also confirmed that higher concentration will give a better corrosion protection. Inorganic inhibitor molecules suppress corrosion by adsorbing to the alloy surface, forming an exterior protective coating that prevents corrosion. The result was confirmed and reviewed by the electrochemical measurements, scanning electron microscopy (SEM) as well as energy dispersive X-ray spectroscopy (EDS).

Keywords: Aluminium Alloy, Inorganic Inhibitor, Corrosion, Electrochemical Measurement, Surface Morphology

PENGARUH PERENCAT PADA PERILAKU HAKISAN AL-MG ALOI

ABSTRAK

Permintaan berterusan untuk penyewaan keluli yang unggul dan cekap terhadap evolusi aluminium asas kepada rangkaian keluli aloi aluminium. Sejak itu, aloi aluminium telah digunakan dalam banyak aplikasi kejuruteraan seperti bahagian enjin, aplikasi marin, dan aplikasi lain menuntut sebilangan besar aloi aluminium. Walau bagaimanapun, Al-Mg terdedah kepada serangan berterusan dari kakisan, oleh itu penggunaan perencat kakisan diperlukan untuk meningkatkan ketahanan kakisan Al-Mg. Tujuan penyelidikan ini adalah untuk mengkaji kesan perencat anorganik terhadap Al-Mg dalam media korosif serta mengkaji morfologi permukaan Al-Mg dengan atau tanpa perencat anorganik.

Ujian kakisan elektrokimia dilakukan pada aloi Al-Mg dengan pelbagai jenis media korosif dan perencat bukan organik. Mekanisme kakisan dengan atau tanpa dihambat pada Al-Mg diperhatikan oleh kajian polarisasi potensiodinamik. Analisis morfologi struktur mikro dilakukan dengan menggunakan mikroskop elektron imbasan (SEM) bersama dengan spektroskopi sinar-X penyebaran tenaga (EDS). Hasil tinjauan ini menunjukkan bahawa Al-Mg terhakis teruk di bawah media korosif berasid kerana ion yang agresif. Penambahan perencat bukan organik seperti kromat, molibdat, fosfat dan nitrat terbukti dapat mengurangkan kadar kakisan aloi Al-Mg. Hasilnya juga mengesahkan bahawa kepekatan yang lebih tinggi akan memberikan perlindungan kakisan yang lebih baik. Mekanisme perencatan dari molekul perencat anorganik dengan penjerapannya ke permukaan aloi, mewujudkan filem pertahanan luaran yang menghalang kakisan. Hasilnya disahkan dan ditinjau oleh pengukuran elektrokimia, mikroskop elektron imbasan (SEM) serta spektroskopi sinar-X penyebaran tenaga (EDS).

Keywords: Aloi Aluminium, Perencat Anorganik, Hakisan, Ujian Elektrokimia, Morfologi Permukaan

In Honour of My Father and Mother, Ir. Dr. Mohd Adly and Sarimah Hassan.

"Honour Thy Father and Thy Mother, That Thy Days May Be Long Upon the Land Which the Lord Thy God Giveth Thee" – Exodus 20:12

ACKNOWLEDGEMENT

First and foremost, I praised ALLAH S.W.T, the almighty creator who led me to go through the most difficult time of my thesis writing with His profound and unconditional love, along with the blessing from both of my parents with their support and dua' to make this success. For it to be a success also required a lot of guidance and assistance. Along the process of completion of my thesis, it has been done under supervision and assistance from the people whom I would like to thank them.

I would like to express my truthful appreciation and respect my supervisor Dr. Nazatul Liana for giving me trust and opportunity to complete the project with the guidance and a non-stop support which made me complete every task appropriately. Although she had a busy schedule managing the Ph.D. student, yet still providing such nice support and guidance which I am here to give the highest gratitude to her.

I also owe my deep appreciation to all the lecturers and my classmates for their endless friendship and encouragement contributing moral support and all the invaluable contribution until the completion of this research during this pandemic.

TABLE OF CONTENTS

LIST OF FIGURES

LIST OF TABLES

CHAPTER 1: INTRODUCTION

1.1 Background

The technological constructions of materials used in modern automobile and machinery have advanced significantly during the last decade. The development and manufacture of the next generation technology is compelled by the imperatives of safety, emission control of dangerous combustion products, and comfort while simultaneously reducing the mass of the mechanization. Although advancements in the field have been made, demand for the structures remains high, which incorporate ever with lighter materials which necessitating continuous development and study in this subject.

Aluminium and aluminium alloys have been widely adopted and found in such diverse industries as aerospace, automotive, shipbuilding, high-speed rail especially in their structural components due to their exceptional mechanical properties (Stojanovic et al., 2018). Particularly, aluminium possessed the power-to-weight ratio, high damage tolerance, economical, good wear resistance and to some degree, its corrosion resistance. In addition, simple and cost-effective technologies for producing most aluminium alloys are required for continued application expansion. Aluminium and its alloys possessed several advantages such as flexibility, cost-effective, and appealing metallic materials for a variety of applications. Aluminium alloys are second only to steels in terms of structural metals. (Davis, 1999a). Creating a composites with two or more types of improvements to increase the mechanical characteristics of the basic alloy is one of the most successful techniques of increasing the properties of aluminium alloys. From a corrosion standpoint of this review study, aluminium has shown to be a successful material in a variety of applications ranging from commodity roles to aviation structural components. A variety of aluminium alloys can be successfully used in environmental/atmospheric conditions in their typical form, allowing the corrosion protection sector to concentrate on meeting market demands in more demanding applications such as those that require coating systems, such as the aerospace industry (Sukiman et al., 2013).

Despite being the most well-known alloy, the demand with better mechanical properties such as strength, good formability, weldability, and high corrosion resistance, thus, the 5XXX series alloys (Al-Mg) were first developed in the 1930s in response to the needs. The difficulties face more than a decade is maintaining the aluminium alloy in harsh condition, which to these days the China Rails High-speed is one of the example that facing this issue (Fan et al., 2020). It is vital to estimate corrosion properties systematically in the development of advanced Al alloys and the design of products to build foundations for interactive corrosion management. It is advised that the Composition-Processing-Microstructure-Property-Performance relationship be considered throughout the lifetime of Al alloys (Fan et al., 2020). When targeting their corrosion resistance, perspectives such as solid solution strengthening, dispersion/precipitation strengthening, work hardening, and grain refinement, as well as their combinations, should be double verified since corrosion behaviour of material is influenced by a variety of parameters, including composition, processing, and microstructures which will have the greatest influence on pitting, IGC, exfoliation, and SCC (Sukiman et al., 2013). Multiple ageing treatments, in particular, are thought to be a successful processing procedure for achieving desirable effects on characteristics like the SCC of specific alloys (Fan et al., 2020). On the one hand, solute and precipitation segregation at grain boundaries may result in lower toughness and increased susceptibility to IGC in service. Solutes used for precipitation hardening, on the other hand, may reduce toughness and fatigue characteristics while also causing corrosion pits. The Zn/Mg atomic ratio has been addressed as an important aspect in the development of improved high-strength Al alloys with outstanding resistance to SCC and IGC due to the high dissolution rate of active particles - MgZn2. Similarly, in Al-Mg-Si-Cu alloys, the Mg/Si atomic ratio has a crucial role in controlling the type and content of second phases, particularly in preventing the production of the hazardous component phase b-Al Fe Si (Fan et al., 2020).

Despite all of the cons, pure aluminium exhibits excellent corrosion resistance due to the creation of a layer oxide coating that is durable, bound to its surface (passive layer) and, if destroyed, restores promptly in most situations which is termed as re-passivation (Davis, 1999b). This protective oxide layer is particularly stable in near-neutral solutions of most non-halide salts. As a result, these solutions have superior pitting resistance. Nonetheless, aluminium is sensitive to pitting corrosion in open air solutions containing halide ions, the most common of which is Cl-. The alloys utility is limited due to its high vulnerability to corrosion in chloride (Cl-) containing environments, which is caused by the presence of intermetallic particles (IMPs) with a different electrochemical potential than the alloy matrix (Rodič et al., 2019) because the metal is rapidly polarised to its pitting potential in the presence of oxygen and due to Cl- promote the growth of soluble chlorinated aluminium hydroxide, thus inhibits the creation of a stable oxide on the aluminium surface.

Corrosion is a major issue that drains firm earnings. The annual cost of battling corrosion is estimated to be $1 trillion which Corrosion-related total costs comprise the cost of design and building or manufacturing, the cost of corrosion-related maintenance, repair, and rehabilitation, and the cost of depreciation or replacement of structures rendered unsuitable by corrosion (Brycki et al., 2018). This is a problem that industries are continually confronted with, and they are constantly looking for solutions to limit the losses. The greatest approach to avoid corrosion is to avoid it in the first place. Experts in anti-corrosion utilise a variety of strategies to prevent corrosion, one of which is the application of various types of corrosion inhibitors. Thus, a practical and effective approach of controlling corrosion of certain aluminium alloys is through the application of corrosion inhibiting agents are introduced. A corrosion inhibitor, by definition, is a chemical agent that, when added in small amounts to an environment, significantly reduces the rate of corrosion disruption of a process. An evaluation of this improvement can be used to determine an inhibitor's effectiveness. From the previous research, it was found that the application of inhibitors reduces the rate of corrosion, but the result varied depending on the type of inhibiting agents that applied. Inhibitors have historically been regarded the front-liner against corrosion in the engineering industries and marine applications. Corrosion inhibitors have been the topic for a large number of scientific research. The majority of the outcome occur from trial-and-error experiments, both in the field and in the laboratories. There are several rules, equations, or hypotheses to govern inhibitor development or use (Godínez et al., 2003).

Various scholars have categorised inhibitors in different ways. Some authors prefer to categorise inhibitors according to their chemical functions and some depending on their mechanism, application, or chemical nature. Thus, in terms of chemical functionality can be expressed in the following manner, inorganic inhibitor, organic anionic and organic cationic. Corrosion inhibitors, however, are the most regrouped into an organisation structure according to their functionality such as passivating (anodic), cathodic, organic, precipitation inhibitors and volatile corrosion inhibitors. A four distinct types of environments are concerned in the majority of inhibitor applications , for instance, natural waters, supply waters, aqueous solutions of acids, industrial cooling waters, etc of which corrosion mechanisms are described in the following sections in terms of these primary environments (Godínez et al., 2003).

In many engineering applications, corrosion is one of the most common causes of failure. It is important to note that corrosion inhibitors are one of the most effective solutions for preventing corrosion from occurring; therefore, determining which type of inhibitor to use is critical in order to avoid corrosion failure. This protects the steel from corrosion while also lowering the maintenance costs. Several studies have discovered that the inclusion of inhibitors can further improve the protection against corrosion attack. After all is said and done, the outcome of efficacy varies from one individual to another. This information will be discussed in greater depth in the literature review, which will be presented in the following part, in order to acquire data on every aspect of the preceding result.

1.2 Research objectives

i. To examine the effect of concentration of inorganic inhibitor on the corrosion behaviour of 5xxx series of aluminium alloy (Al-Mg).
ii. To characterise the surface morphology of 5xxx series of aluminium alloy (Al-Mg) under corrosive media with or without inorganic inhibitors.

1.3 Scope of research

The primary goal of this review is to investigate the corrosion behaviour of aluminium alloy 5xxx series (Al-Mg) with and without the inclusion of inorganic inhibitors under corrosive media. A review of the corrosion behaviour of these steel samples was conducted using potentiodynamic polarisation method, as well as scanning electron microscopy (SEM) for the observation of changes in the micro-morphology of the steel samples. According to the microstructure of the material, its corrosion resistance will be determined, and the change in grain size of the steel will be observed using a scanning electron microscope. Finally, after the review study is completed, the evaluation of inorganic inhibitor performance on Al-Mg steel generally concluded on its efficacy.

1.4 Outline of dissertation

A total of five chapters makes up this dissertation. The first chapter presents a brief overview of this study project, including the research background, aims, and scope. The second chapter provides a thorough discussion of the literature background study for this topic. In chapter three, the experimental methods used to evaluate the corrosion behaviour with or without inorganic inhibitor in Al-Mg are described. This chapter covers the equipment utilised, sample preparation procedures, electrochemical corrosion measurement methodologies, and corrosion product characterization procedures. The results of the review study are reported in Chapter 4, which are examined and compared reciprocally. This chapter delves into the findings. The fifth chapter concludes the research findings and makes recommendations for future research.

CHAPTER 2: LITERATURE REVIEW

2.1 Aluminium

Aluminium a silver-white metallic element abbreviated as Al is a material that belongs to group III of the periodic table with the structure composition of $1s^2 2s^2 2p^6 3s^2 3p^1$. With a density of $2.7 \mathrm{g/cm^3}$, a cubic foot of aluminium weighs just an approximate of 78 kg compared to a cubic foot of steel weighs about 222 kg, indicating that aluminium is about one-third the mass of steel ($7.83 \mathrm{g/cm^3}$), proof to its light weight, coupled with the high strength of particular aluminium alloys, the steel structure was outperformed, allows for the design and construction of strong, lightweight structures that are particularly helpful for moving objects, such as spacecraft and aircraft, as well as all forms of land and water-based vehicles (Davis, 1999a; Sukiman et al., 2013). The physical properties of aluminium are shown in the Table 2.1 as follows.

Table 2.1 : Physical properties of pure aluminium. (Sanders, 2012)

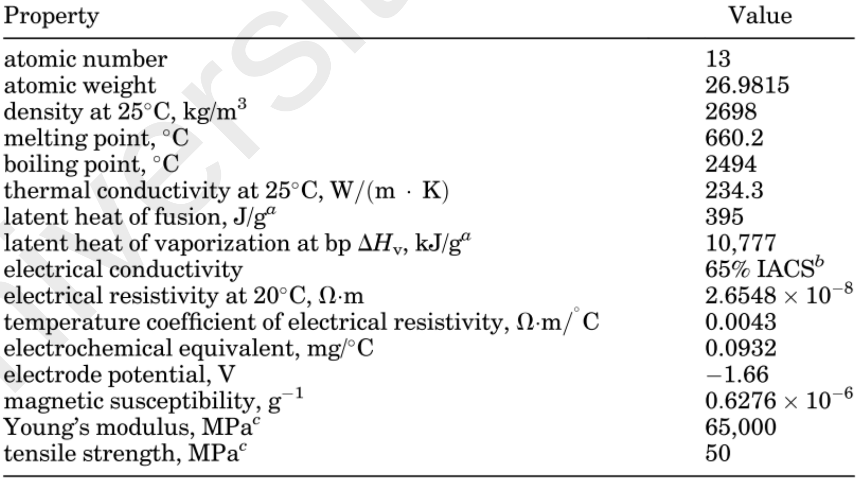

Property	Value
atomic number	13
atomic weight	26.9815
density at 25°C, $\mathrm{kg/m^3}$	2698
melting point, °C	660.2
boiling point, °C	2494
thermal conductivity at 25°C, W/(m · K)	234.3
latent heat of fusion, $\mathrm{J/g}^a$	395
latent heat of vaporization at bp ΔH_v, $\mathrm{kJ/g}^a$	10,777
electrical conductivity	65% IACS^b
electrical resistivity at 20°C, Ω·m	2.6548×10^{-8}
temperature coefficient of electrical resistivity, Ω·m/°C	0.0043
electrochemical equivalent, mg/°C	0.0932
electrode potential, V	−1.66
magnetic susceptibility, g^{-1}	0.6276×10^{-6}
Young's modulus, MPa^c	65,000
tensile strength, MPa^c	50

Aluminium is the most abundant metal on Earth, in fact, accounting for almost 8% of the planet's core mass (Sanders, 2012). After oxygen and silicon, it became the most common element on earth, placed in third. Pure aluminium, on the other hand, does not exist in nature since it easily binds with other elements. This is one of the reasons why it was only recently discovered. The ironic thing about aluminium is that it should not be all that useful in the first place. It is this type of reaction that causes iron to rust that causes the metal to oxidise or lose electrons rapidly. According to the analyst from University of Wisconsin, unlike flaky iron oxide, the product of this reaction, aluminium oxide, adheres to the parent metal, preventing it from further degradation, and therefore protecting it (Davis, 1999a). Pure aluminium, on the other hand, does not exist in nature due to its proclivity for forming bonds with other elements. This is one of the reasons why it was only recently discovered and studied.

Aluminium was first produced in 1824, but it took another fifty years for people to figure out how to generate it on a sufficient scale for industrial use in the great economic development. In nature, aluminium sulphates are the type of aluminium that are commonly encountered whereas these are minerals that contain alkaline metal such as lithium, sodium, potassium, etc, while the other based on a metal from the periodic table's third group, mainly aluminium which considered to be the combination of two sulphuric acids. Aluminium sulphates are still utilised today in various applications, including water purification, cooking, cosmetics, in the pharmaceutical business, and in other fields. Aluminium was named from aluminium sulphates, which were called alumen in Latin. In today's world, researchers are aware of almost 300 different aluminium compounds and minerals that contain aluminium, ranging from feldspar, which is a major source mineral on the planet, to ruby, sapphire, and emerald, which are significantly less common. However, regardless of how prevalent aluminium may be, it may have remained concealed for all time if it had not been for the invention of electric current. When scientists discovered that they could utilise electricity to break down chemical compounds into their constituent elements, they realised that they had discovered aluminium. Christian Oersted, a Danish physicist who lived in the nineteenth century, discovered how to make aluminium by electrolysis. Electrolysis, often known as electrolytic reduction, is a method that is still being used today to manufacture aluminium alloys.

On top of that, bauxite a very common mineral, is now the principal raw ingredient in the manufacturing of aluminium. Bauxite is a clay mineral composed of various range of aluminium hydroxide combined with iron, silicon, titanium, sulphur, gallium, chromium, vanadium oxides, sulfuric calcium, iron, and magnesium carbonates. Bauxite is found in the earth's crust and can be found in the ocean. In other words, the normal bauxite comprises over half of the elements in the periodic table. Furthermore, because of the appearance of bauxite, roughly a hundred years ago, aluminium was sometimes referred to as silver extracted from clay because of the way it looked. In order to make one tonne of aluminium, approximately 4 to 5 tonnes of bauxite are required. Bauxite is processed into alumina, or aluminium oxide Al_2O_3, in the initial stage of aluminium manufacturing which Bayer filed a patent the method to extract it in 1887 (Vargel et al., 2020). Alumina appears as a white powder, and it is electrolytically reduced into aluminium in aluminium smelters. Either aluminium is extremely hot or extremely cold, pressure can be used to process it quickly and efficiently. It is capable of being rolled, dragged, and stamped. In fact, it does not require special paint (coatings), fire retardant, and is non-toxic, unlike plastics. It is also extremely flexible, allowing it to be utilised to manufacture sheets as thin as 4 microns and ultra-thin wire. Aluminium can be manufactured into ultra-thin foil that is three times thinner than a human hair. Aluminium indeed less expensive as compared to other materials. The fact that aluminium readily in compounds form with other chemical elements has led to the development of an enormous range of aluminium alloys as previously mentioned. In some cases, even a very little amount of admixtures can significantly alter the physical properties of a metal, allowing it to be applied in various new area.

Aluminium is essential to the modern building, automobile, aviation, energy, food, and other sectors. Without it, none of these would be conceivable. Furthermore, aluminium has emerged as a symbol of advancement across a vast expanse of the world. The combination of characteristics listed above would appear to be sufficient to make aluminium the material of choice in industry but, there is another virtue that is equally important in which aluminium can be reused over and over again. Metals such as aluminium and its alloys can be melted down and reused without affecting their mechanical characteristics in the process. Experts have noted that one kilogramme of recycled aluminium cans can save up to 8 kilogrammes of bauxite, 4 kilogrammes of different fluorides, and up to 15 kilogrammes of power each kilogramme of aluminium cans recycled (Sanders, 2012). A total of approximately 75% of the aluminium produced over the period in which the aluminium industry has operated is still in use today.

2.2 Aluminium alloys

On the contrary, the capability of an aluminium itself is not sufficient to conclude as a whole, because a pure aluminium can be transformed further into an advanced material when other elements are introduced as it is known as aluminium alloy. In chemistry, an aluminium alloy is a chemical composition in which other elements are combined with pure aluminium to improve its qualities, precipitation hardening, control of matrix microstructure, notably its strength (K.Sankaran & S.Mishra, 2017). Iron, silicon, copper, magnesium, manganese, and zinc are among the additional elements included in the alloy, and their combined amounts may account for as much as 15 percent of the alloy's total weight. In order to fabricate aluminium alloy, it must be thoroughly mixed with the other elements when the aluminium is still in the molten or liquid state. Several facts to understand about Al alloy in which the qualities of aluminium, such as its strength, density, workability, electrical conductivity, and corrosion resistance, are altered when other elements, such as magnesium, silicon, or zinc, are added to the alloy. Secondly, two different aluminium alloys are used on most of the military vehicles such as the 5xxx series and the 7xxx series which will explain later on each category, indeed, the materials which are trusted to keep soldiers safe and mobile, are also utilised in a wide range of other military vehicles. Third, the aluminium can, which is widely used as a beverage container in the United States, is composed of several different aluminium alloys. The shell of the can is made of 3004 aluminium, and the lid is made of 5182 aluminium. It is sometimes necessary to use more than one alloy to create a single daily object. Finally, strength of the aluminium alloys can be enhanced by cold working or heat treatment. Contribution of the additives and treatment used in making each alloy, results in a unique set of characteristics.

Alloys are characterized by a four-digit (xxxx) number, with the first digit describes a general class or series, of alloys that is distinguished by the principal alloying elements used in the alloy (Kaufman, 2000). Every digit has its own connotation in which the principal alloying class of the series begins with that number is defined by the first digit. The second digit is range from zero (original composition) to a certain value which denotes the variations in the original basic alloy. Variations are often described as 0.15% to 0.50% or greater changes in one or more alloying elements, depending on the degree of the additional element. The last two digits, third and fourth numbers denote the specific alloy within the series; the values of those digits have no particular importance, and they are not always used in that order (Davis, 1999a; K.Sankaran & S.Mishra, 2017; Kaufman, 2000; Sukiman et al., 2013). The main alloying elements designation system can be referred in Table 2.2 below.

Table 2.2: The Aluminium Alloys numbering system designation. (Davis, 1999a; Kaufman, 2000)

Alloy system	**Aluminum series**
Work-hardenable alloys	
Pure Al	1*xxx*
Al-Mn	3*xxx*
Al-Si	4*xxx*
Al-Mg	5*xxx*
Al-Fe	8*xxx*
Al-Fe-Ni	8*xxx*
Precipitation-hardenable alloys	
Al-Cu	2*xxx*
Al-Cu-Mg	2*xxx*
Al-Cu-Li	2*xxx*
Al-Mg-Si	6*xxx*
Al-Zn	7*xxx*
Al-Zn-Mg	7*xxx*
Al-Zn-Mg-Cu	7*xxx*
Al-Li-Cu-Mg	8*xxx*

Table 2.2, it specifies a group of wrought alloys in which every aluminium series is differentiated into two sub-group, which are work-hardenable alloys (non-heat treatable) and precipitation-hardenable (heat treatable) alloys. Not only alloys are classified as abovementioned, but also practically divided into two main categories shown in Figure 2.1, cast and wrought alloys.

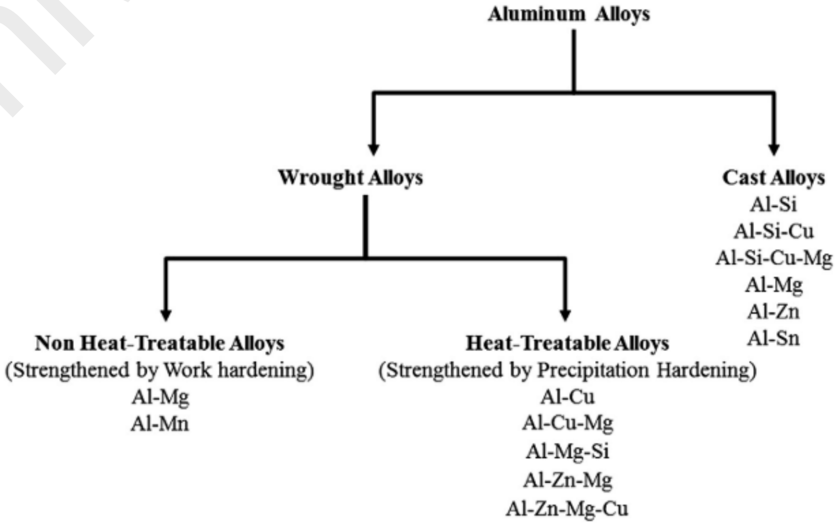

Figure 2.1: Two main classifications of Aluminium Alloys. (K.Sankaran & S.Mishra, 2017)

The full categories of aluminium alloys are illustrated in Figure 2.1. It is worth noting that the alloy compositions listed in Figure 2.1 above only contribute a small portion of the overall number of compositions created. The Aluminum Association Inc. has registered over 500 alloy designations/compositions for aluminium alloys (Davis, 1999a). Apart from the particularize every alloy series, this review paper is more focused towards the 5xxx series of aluminium alloy. Most studies have relied on 2xxx, 6xxx, 7xxx series alloy because it is traditionally been the most extensively researched (Poznak et al., 2018), thus, lacking in the scientific literature for 5xxx series of aluminium alloy.

2.2.1 5xxx series alloy

The 5xxx family aluminium alloys are used in a wide range of applications, ranging from shipping containers to boats, which are their most common use. The features of the 5xxx series of aluminium alloy make it the best building material for all maritime related, whether it is a leisure boat, commercial ship, or navy vessel as a result of their excellent strength-to-weight ratio, corrosion resistance, and weldability. Before delving into the specific advantages of the 5xxx series and its uses, simply put, the 5xxx series is identified by the presence of magnesium as its primary agent, which confers high strength as well as excellent weldability among other properties on the alloy (Choi et al., 2018). Table 2.3 below shows the standard composition of 5xxx series of Al-Mg.

Table 2.3: The composition of 5xxx series of Al-Mg in wt%. (Choi et al., 2018)

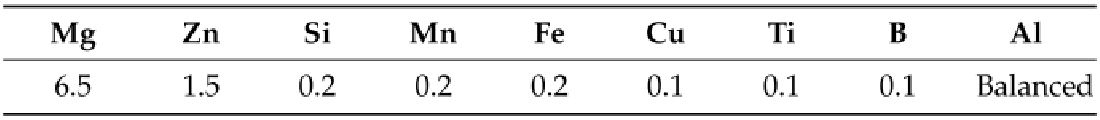

Mg	Zn	Si	Mn	Fe	Cu	Ti	B	Al
6.5	1.5	0.2	0.2	0.2	0.1	0.1	0.1	Balanced

Alloying elements are added to wrought alloys in amounts ranging from 1 to 7 wt%, meanwhile, in certain cases for casting alloys, up to 20 wt% silicon (Vargel et al., 2020). For 5xxx series aluminium alloys, magnesium (Mg) is the most important alloying element in this group of elements as the addition of magnesium (Mg) is up to 6.5 wt%. In order, to achieve solid solution hardening, magnesium is added into the alloys. Minor alloying elements like as zinc (Zn), silicon (Sn), titanium (Ti), manganese (Mn), beryllium (Be), iron (Fe), and copper (Cu) are added as alloys of the 5xxx series and act as agents for weldability improvement. However, stress corrosion cracking (SCC) and intergranular corrosion (ICC) are more likely to occur when 3% or more of magnesium is added to the Aluminium thus, in the $\beta(Al_3Mg_2)$ phase, which forms continually at the grain boundaries, is responsible for these phenomena (Choi et al., 2018). For many years, the industry and researchers have been very concerned about the growth of the secondary phase (Al_3Mg_2) in the material and this matter will be discussed later in section 2.5.

The 5xxx series alloys can be divided into two sub-group as shown in Figure 2.1 which are wrought alloys and cast alloys. The 5xxx series aluminium system is described as a non-heat treatable alloy that obtains the majority of its strength from cold rolling and solute solution hardening, as opposed to heat treatable alloys like the 2xxx, 6xxx, and 7xxx series, which rely mainly on precipitation hardening to achieve required mechanical strength (Unocic et al., 2008). Owing to the lower amounts of solute in the 5xxx series, it is deemed non-heat treatable, nevertheless, alloys with higher quantities of Mg can also become heat treatable. While alloying with magnesium improves strength, the most significant effect is magnesium (Mg) tendency to promote work hardening in the alloy (Daniel Scotto D’Antuono, 2017). Moreover, the Holloman-Stumpf equation is closely related to the relationship between ultimate tensile strength and the amount of strain hardening supplied by magnesium (Mg) additions where the following impacts are shown in the illustration below.

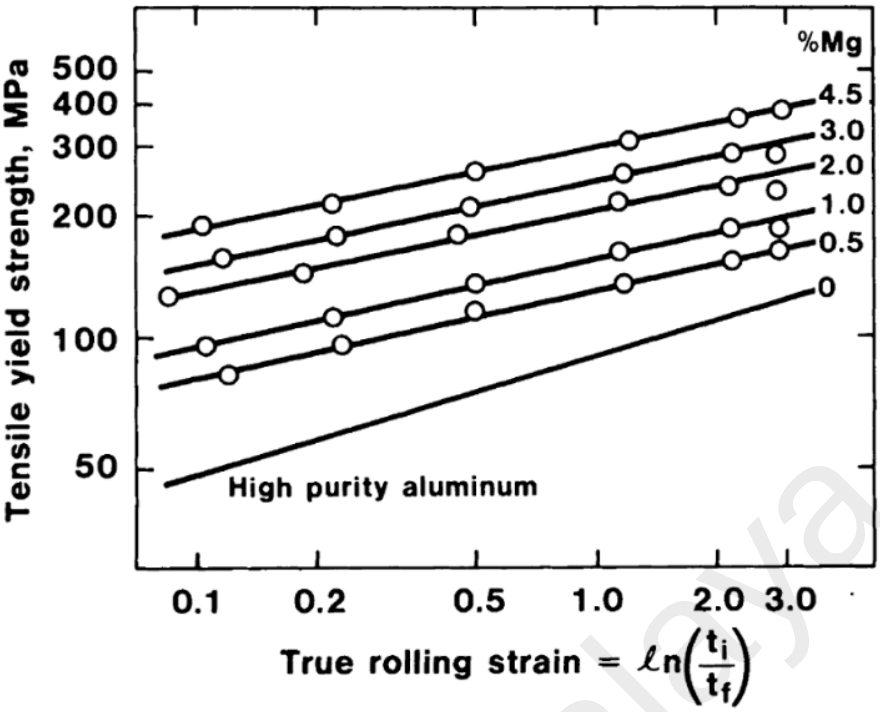

Figure 2.2: The high purity and Al-Mg binary alloys of strain hardening during cold rolling. (Ryen et al., 2006)

According to Figure 2.2, it can be seen that the capacity of the alloy to work harden rises as more magnesium is injected into it, and hence the tensile yield strength rises exponentially as well. This has resulted in cold rolling being a highly typical processing method, as well as alteration of the magnesium concentration of steel (John E. Hatch, 1984). However, when it comes to the 5xxx series alloy system, it is assumed to be a binary system, also known as a binary compound, which is a chemical complex that contains two distinct elements in the field of materials science. As depicted from phase diagram in Figure 2.3, there are only a few possible equilibrium phases.

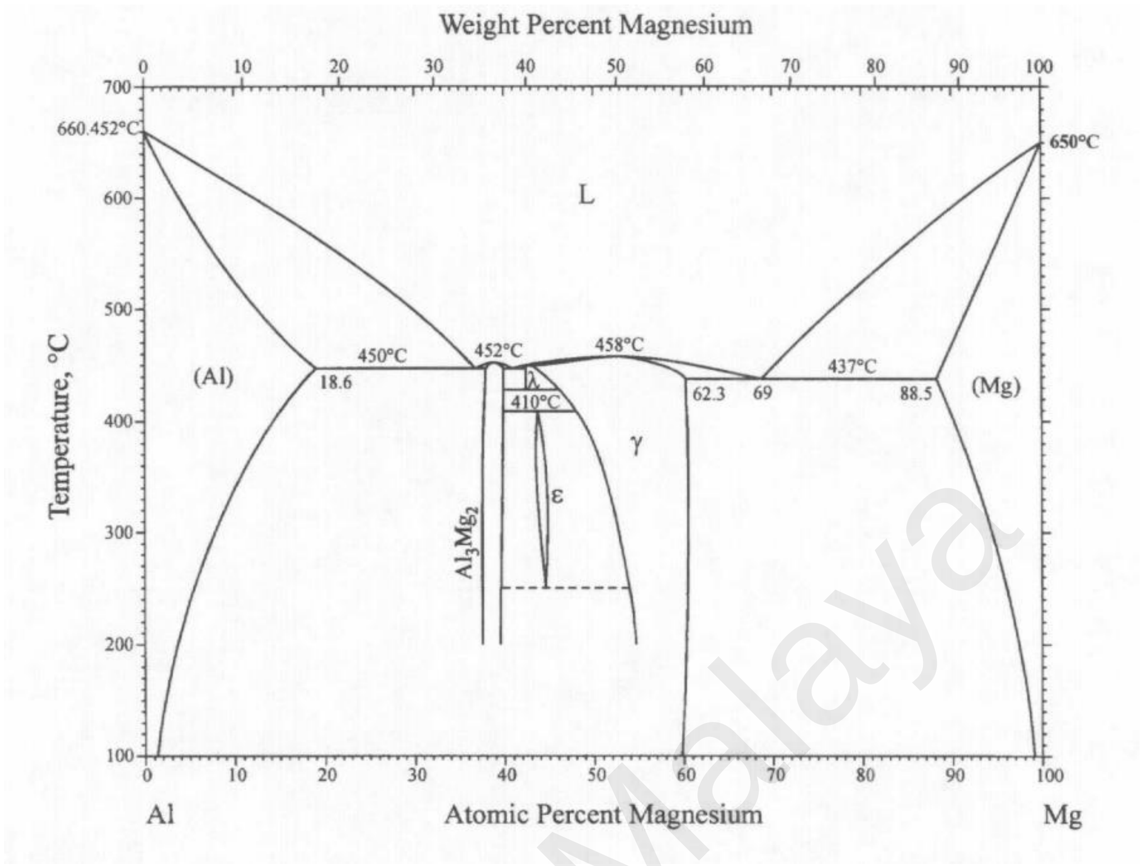

Figure 2.3: The phase diagram of Al-Mg. (Okamoto, 1998)

The phase diagram is not too intricate as it illustrate and clearly demonstrate the phases of equilibrium indicated within the plot where solid solutions of Aluminium (Al) and magnesium (Mg) are located on the left and right, $\mathrm{Al_3Mg_2}$ (β phase) compound at 37 wt% of atomic percent magnesium (Mg), and γ represents a $Al_{12}Mg_{17}$ compound (Okamoto, 1998; Unocic et al., 2008). The detailed interpretation on the phase diagram explains that the precipitation occurred in Al+β phase is viable at temperature from 20℃ to 450℃ at the atomic percent magnesium (Mg) concentration starting from approximately 1wt% to 37wt%. As the concentration of Mg increases, the solvus temperature rises with it, and resulting in a positive slope, thus, indicating a higher probability of precipitation to form (Smallman & Ngan, 2013). Usually, the most used concentration of Mg in industrial application maintains around 4wt% to 5wt% to avoid the loss of ductility and allows for secondary precipitation when exposed to high temperatures. Sensitization is the term for the process of secondary phase precipitation.

2.2.2 Sensitisation/Tropicalization of Al-Mg 5xxx Series

Alloy sensitization refers to the precipitation of carbides at grain boundaries that causes the steel or alloy to be prone to intergranular corrosion or intergranular stress corrosion cracking when it is exposed to high temperatures (Searles et al., 2002). Beginning with supersaturated solution (SSS) which contain >3% of magnesium (Mg), the Mg segregation process eventually leads to the formation of the β equilibrium phase (Lathabai & Lloyd, 2002; Nebti et al., 1995; Starink & Zahra, 1998; Yassar et al., 2005) .The formation of the β equilibrium phase can be illustrated in Figure 2.4 as follows:

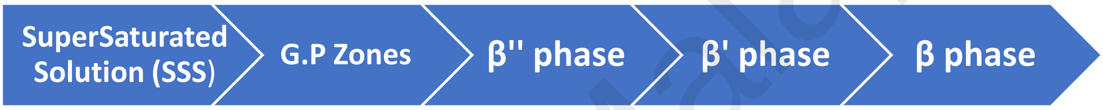

Figure 2.4: The formation process of β equilibrium phase. (Nebti et al., 1995)

The formation of G.P zone and β” phase will not be discussed in this review since the 5xxx series of aluminium alloy contain <6 wt% of magnesium (Mg) since GP zones and β” phase are more likely to be formed in materials that have 13 wt% of magnesium (Mg) or more, hence, G.P zone and β” phase formation infrequently seen in alloys with lower Mg concentrations (Starink & Zahra, 1998). Some researchers have indicated that these early-stage precipitates can be formed in β’ phase, yet the β equilibrium phases, are the key phases of interest. The exact mechanism of nucleation and growth is unknown, but the phase formation is usually temperature dependent (Yi et al., 2017). Both β' and β precipitations can occur from the SuperSaturated Solution (SSS), as seen in the Figure 2.4 above, with the β' phase emerging first and leading to the development of β phase equilibrium. The β' phase is the lower temperature precipitate, while the β phase equilibrium is the higher, and their coexistence has been documented on occurrence (Daniel Scotto D’Antuono, 2017). According to Hamana et al. (2004) the SuperSaturated Solution (SSS) normally converts into a state of β phase equilibrium by β’ phase beforehand, however, at accelerated timelines with high temperature, the production of a state of β equilibrium from the SuperSaturated Solution (SSS) has been demonstrated to be attainable. It is vital to comprehend the precipitation process of β phase equilibrium in order to form a clear image of the phenomenon.

Zhang et al. (2016) investigated the presence of β phase equilibrium as illustrated in Figure 2.5 and the formation of grain boundary β phase (Al_3Mg_2) on the material in corrosive environment which led to the intergranular corrosion cracking (IGC) and stress corrosion cracking (SCC). As seen in Figure 2.5a, the arrow indicates the substantial amount of grain boundaries β phase appeared after being sensitized at 100℃ for 90 days. For Figure 2.5b, the image shows grain boundaries β phase appeared after being sensitized at 70℃ for 30 months which proved the β phase appeared above temperature above 50℃.

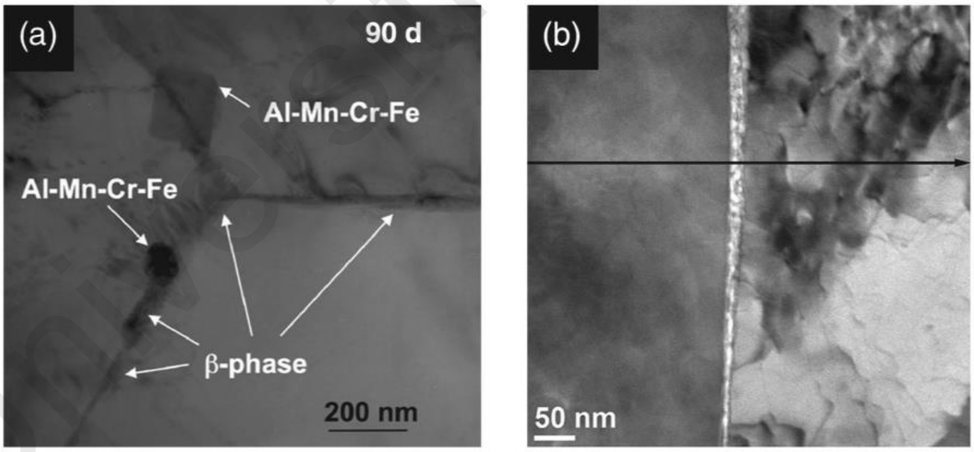

Figure 2.5: Example of β phase in aluminium alloys. (R. Zhang et al., 2016)

The most reported phase in the documented in the scientific literature is said to be β phase equilibrium. With a lattice value of 28.2 angstroms, the phase adopts a face cubic centred (FCC) structure as shown in Figure 2.6. Yakun Zhu (2013) mentioned that the growth was reported to be incoherent with respect to the grain boundaries and occurs at temperatures in the range of 200°C - 300°C, with dissolution occurring approximate temperature of 400°C (Unocic et al., 2008) , depending on the percentage of magnesium (Mg). Precipitation happened frequently in a heterogeneous approach, similar to that of β' phase, but it is was claimed to appear at later stages of ageing (Unocic et al., 2008).

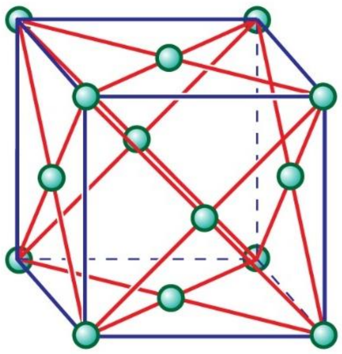

Figure 2.6: Face cubic centered (FCC) of Aluminium.(Yakun Zhu, 2013)

Also, Nebti et al. (1995) and Starink & Zahra (1998) indicated that the composition was very similar to that of β' phase being Al_3Mg_2, although the crystal structure of β and β' phase were different. Somehow, the composition of both β and β' phase as Al_8Mg_5 (Mazurkieicz, 1983) in the early research could be a little misleading. Regardless of the heat treatment application to a given material, the majority of studies only reported β equilibrium phase precipitation.

2.3 Corrosion Inhibitor

As revealed in the previous section, aluminium is often used in ship superstructures and liquid cargo containers because of its light weight and decent strength. Due to their decent strength and corrosion resistance, the 5xxx and 6xxx series aluminium alloys are the most commonly used in harsh environments such as seawater (Nik et al., 2010). As a result, the marine vehicle is exposed to the salty environment owing to not only is the exterior of the cargo containers exposed to corrosive attack, but the inner compartments are also subjected to the effects of corrosive aqueous media. As a result of the exorbitant amount spent on corrosion each year, several approaches and methods have been created to battle corrosion efficiency (Abd El Rehim et al., 2003; Bethencourt et al., 1997). It is a common practice to use inhibitors to prevent corrosion of metals and alloys on the coast and offshore that come into contact with a harsh maritime environment. When compared to other preventive approaches, corrosion inhibitors appear to be appealing due to their low cost and ease of usage. Inhibitors are agents that engage with a metallic surface or the environment to which the surface is exposed to provide a layer of safety to the surface. Inhibitors reduce corrosion by adsorbing themselves to the metallic surface and producing a layer.

Considering the rapid development of industrial applications of these materials, corrosion prevention of Al and related alloys is crucial and hence it is implemented as a part of technological importance. Corrosion inhibitors have traditionally been considered to be the first line of defence against corrosion (Nik et al., 2010). Today, a variety type of corrosion inhibitors that are accessible and suitable for any requirements. A corrosion inhibitor is a "chemical compound that, when present in the corrosion system at a sufficient concentration, reduces the corrosion rate without materially affecting the intensity of any corrosive agent," according to a standard definition by (ISO, 2015). In tiny doses, it is often effective. There are certain exceptions to this rule, including any agent that slows corrosion rate by a significant pH variation, as well as oxygen and hydrogen sulphide scavengers that remove reactive species from the solution (Monticelli, 2018). Corrosion inhibitors are classed as cathodic, anodic, or mixed, as shown in Figure 2.7. The classification depends on whether they hinder the cathodic corrosion process or anodic reactions, or both.

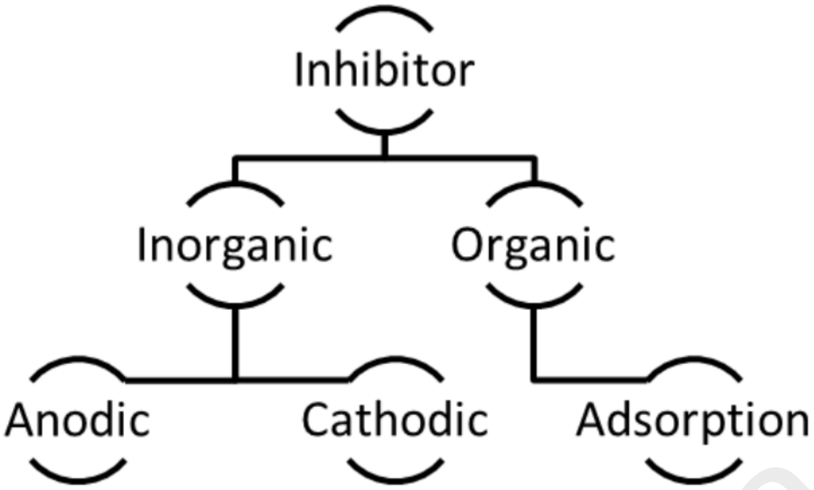

Figure 2.7: Tree diagram of inhibitors classification. (Dariva & Galio, 2016)

To summarize, they either promote a shift in the corrosion potential of the inhibited metal toward the cathodic or anodic directions, or they keep the metal corrosion potential essentially constant. The reduction of a metals active surface area and/or a change in the activation energy of the oxidation or reduction process in corrosion can both impede anodic or cathodic corrosion reactions. When cathodic and anodic corrosion inhibitors are used together, they provide better protection and allow for lower inhibitor concentrations (Corris et al., 2013).

Regardless of which reaction the corrosion inhibitor inhibits, it will generate film by interacting with the metal/solution interface, the mechanism of corrosion inhibition can be anodic, cathodic or a mixture of the two and by adsorption and be simply described in section (i, ii, iii) below. Various scholars have categorised inhibitors in different ways. Some authors prefer to categorise inhibitors according to their chemical functions (Jones, 1989) such as inorganic inhibitors, organic anionic and organic cationic. Although there are other organisational schemes, the most widely used ones involve organising corrosion inhibitors into a functionality scheme, which are as follows:

i. Passivating film (anodic): The corrosion resistance of passivating oxide coatings ranges from 30 to 200 microns. Classic oxidising inhibitors, such as chromates and nitrites, can be found among them, but they have mostly been phased out due to toxicity concerns, which poses a serious threat to human safety.

ii. Precipitation film (cathodic): Chemicals that generate insoluble protective films by reacting with soluble species in the environment or with protected metal ions are known as precipitation film-type inhibitors. These films may be porous and not fully adhering, yet they provide adequate corrosion protection in this scenario.

iii. Adsorption film: Organic compounds are the most common inhibitors that produce adsorption protection coatings. They frequently feature a surfactant-like molecular structure, with a hydrophilic group capable of bonding with metal surfaces and a hydrophobic portion of the molecule projecting toward the solution bulk.

The mechanisms are illustrated in Figure 2.8 below which explained how inhibitor would react on metal. Typically, the efficacy of an inhibitor improves as the concentration of the inhibitor rises. At a concentration of 0.008 percent, a typical excellent inhibitor would provide 95 percent inhibition, while at a concentration of 0.004 percent, it would provide 90 percent inhibition approximately.

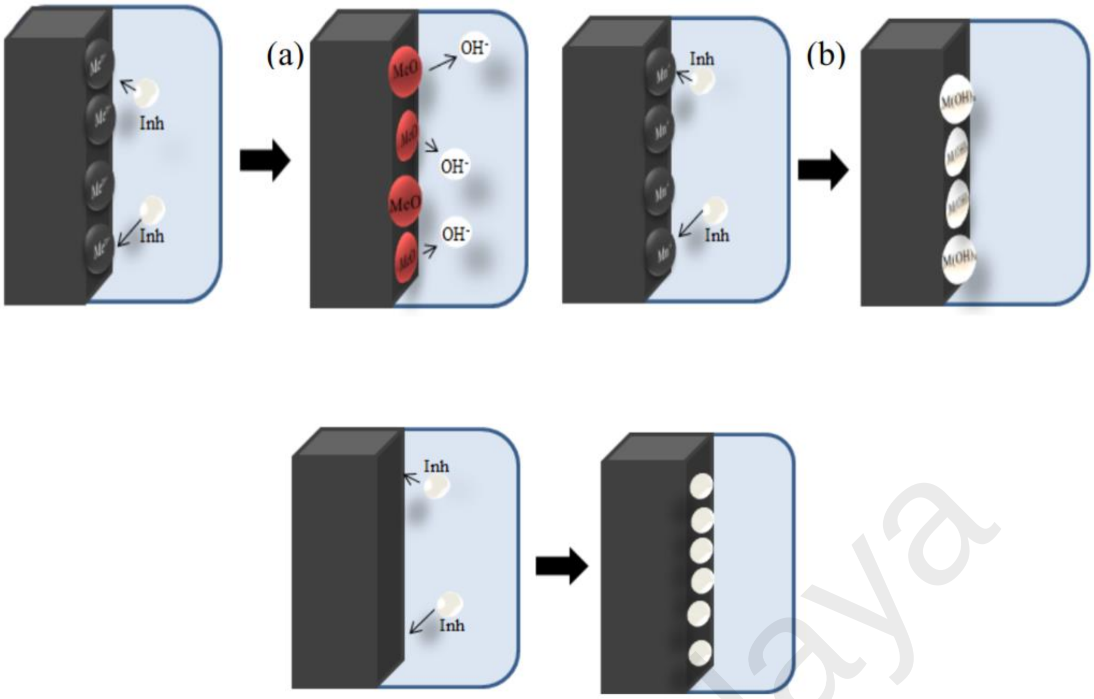

Figure 2.8: The process action of inhibitor shows (a) anodic inhibitors, (b) cathodic inhibitors and (c) adsorption inhibitors. (Dariva & Galio, 2016)

Aside from that, Godínez et al. (2003) explained that the majority of inhibitor application systems for aqueous, or partially aqueous, were concerned with four distinct types of environmental conditions. For example, metal-cleaning operations involving aqueous acid solutions, naturally occurring and treated water in the near-neutral pH range (5 to 9), primary and secondary oil production and atmospheric or gaseous corrosion in restricted spaces are all examples of corrosive conditions. The next subtopic in this review will explain about the inhibitors that related in this review paper in more detail.

2.4 Inorganic Corrosion Inhibitor

Electrochemical reactions in the anodic and cathodic regions are suppressed when inorganic inhibitors are added. Inhibitors are commonly utilized in combination with other chemicals. Zaki Ahmad (2006) mentioned that only at a sufficient level of concentration do these inhibitors react. Organic and inorganic composites are the most often used corrosion inhibitors, with organic inhibitors reducing corrosion by adsorption techniques and inorganic inhibitors preventing corrosion by reacting with the anodic or cathodic elements of the process (Tiu & Advincula, 2015; Umoren et al., 2015). In this section, special attention should be paid to inorganic inhibitors in line to this review paper. Inorganic corrosion inhibitors, in particular, contain zinc, copper, nickel, arsenic, and other metal salts, with arsenic compounds being the most widely utilised. When utilising inorganic inhibitors, there are benefits as well as drawbacks. One of the benefits is the inhibitors able to work magnificently at high temperatures for extended periods of time and costing less than organic inhibitors. However, the limitation occurs when the acid solutions are stronger than 17% hydrochloric acid, and exhibit high toxicity such as hazardous arsine gas (Kausalya & Hazlina, 2020).

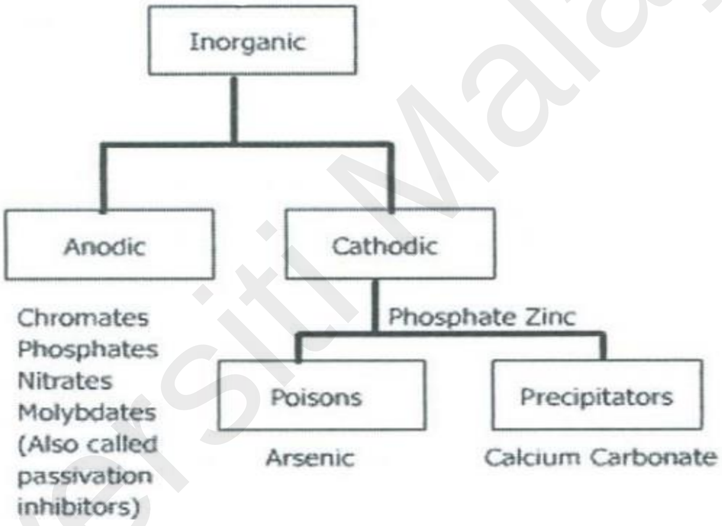

Figure 2.9: List of Inorganic Corrosion Inhibitors of Anodic-Cathodic. (Zaki Ahmad, 2006)

Leaving aside the pros and cons of inorganic inhibitors, there are several inorganic inhibitors that can be addressed. Only the anodic will be covered in this review. In Zaki Ahmad (2006) book, chromates, phosphates, nitrate, molybdates, sulphate, and other inorganic inhibitors are classified as anodic inhibitors, also known as passivation inhibitors. Each of the inhibitors has a distinct specialisation, which will be discussed in greater depth along with the literature. To start with chromate inhibitor, consider to be highly effective inhibitors, however, they are poisonous thus their use is limited and not recommended. In fact, the concentration threshold in industrial water is 120mg/L.

Chromate inhibitors comprise either $Na_2CrO_4/Na_2Cr_2O_7$ as their active ingredient. Iron oxide and chromium oxide are found in the protective passive layer that is created, which makes the chromate inhibitors extremely efficient because of their presence shown in the Figure 2.10 below.

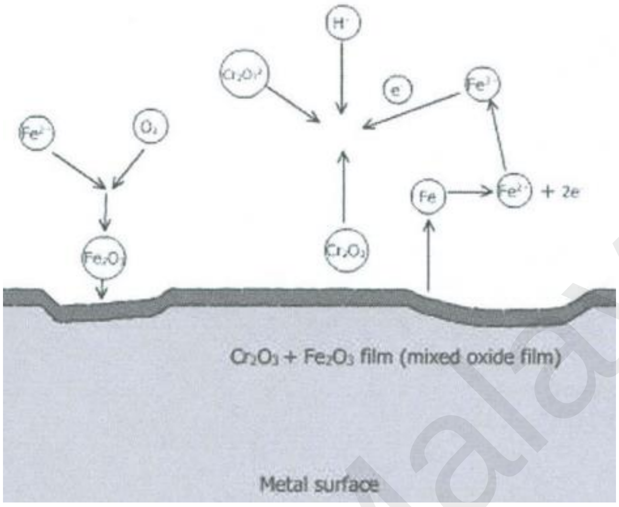

Figure 2.10: action of chromates inhibitor on metal surface. (Zaki Ahmad, 2006)

The reduction of the chromates to form chromium (III) resulting in the reaction at equation 2.1 and 2.2 as follow:

- $Fe \rightarrow Fe^2 + 2e$ (2.1)
- $Cr_4^- + 8H + 3e^- \rightarrow Cr^{3+} + 4H_2O$ (2.2)

The above chemical reaction shows the oxidation of iron and the formation of Cr^{3+}. The oxidation of iron and the reduction of chromium produce a mixed potential that is somewhere in the passivation range, which explains why chromate inhibitor has a passivating effect. However, Frankel & McCreery (2001) explained chromate does not significantly limit the rate of localised corrosion propagation in Al or Al alloys. In the research study of Sehgal et al. (2000) shows under an applied anodic potential, the addition of 0.1 M $Na_2Cr_2O_7$ had no effect on the rate of localised corrosion through AA2024-T3 foils in 1 M NaCl. In reality, chromate inhibitors can operate as an oxidising agent under certain conditions, speeding up the rate of localised corrosion. On the contrary, Sehgal and his team brings the evidence that chromate suppresses the cathodic reaction (especially oxygen reduction) on Al alloys and produces a protective coating that prevents localised corrosion. In one of his studies, the AA2024-T3 in 1 M NaCl buffered with oxygen. Thus, with as little as 10-4 M added $Na_2Cr_2O_7$, the rate of oxygen reduction is clearly slowed (Sehgal et al., 2000).

Following that, the efficiency of nitrites and nitrates varies depending on the type of material being treated. Nitrites are effective inhibitors in a wide range of water types when it comes to iron and several other metals, while nitrates protect solder and aluminium. Both inhibitors are anodic inhibitor that work to prevent the system generate a passive film with ferric oxide works like chromates inhibitors. These are non-toxic and environmentally safe inhibiting agents. At pH levels 9-10, nitrites can also be used to prevent corrosion of copper, tin, and nickel alloys, among other metals. Even so, nitrites and nitrates are not effective if applied in open systems because they will oxidise and decompose into nitrates if there is any oxygen present. The protective coating generated by nitrites can be harmed by the presence of chloride and sulphate ions. Prior to the previous research, Matter et al. (2013) observed the effect of Ce(III) and Ce(IV) as an inhibitive agents into corrosive medium with four (4) different concentration. When compared to the case without the inhibitor, the cerium (III) ions demonstrated stronger inhibitory efficacy than the cerium (IV) ions under very similar conditions (Matter et al., 2013). It has been determined that, of all the rare earth elements, cerium ions have the best corrosion inhibitive efficacy against AA2024 alloy corrosion (Bethencourt et al., 1997; Markley et al., 2011).

Then, there is a phosphate inhibitor which it encourages the formation of protective iron oxide films and by repairing any faults in these films that have occurred. Cerium diphenyl phosphate $\mathrm{Ce(dpp)_3}$ has previously been demonstrated to be a powerful corrosion inhibitor for the aluminium-copper magnesium alloys AA2024-T3 and

AA7075 when exposed to chloride solutions studied by Hill and his teams (2011). When tested in a chloride environment (0.1 M NaCl), the inhibitor $\mathrm{Ce(dpp)_3}$ was found to be an effective corrosion inhibitor on aluminium alloys AA7022, AA7075, and AA7050 (Hill et al., 2011) shown in the optical micrographs Figure 2.11 below. The specimen of (a), (b) and (c) resulted in a considerable reduction in the corrosion rates by adding150ppm of $\mathrm{Ce(dpp)_3}$ as compared to the specimens exposed only in ($0.1\ M\ NaCl$) shown in (d), (e), and (f).

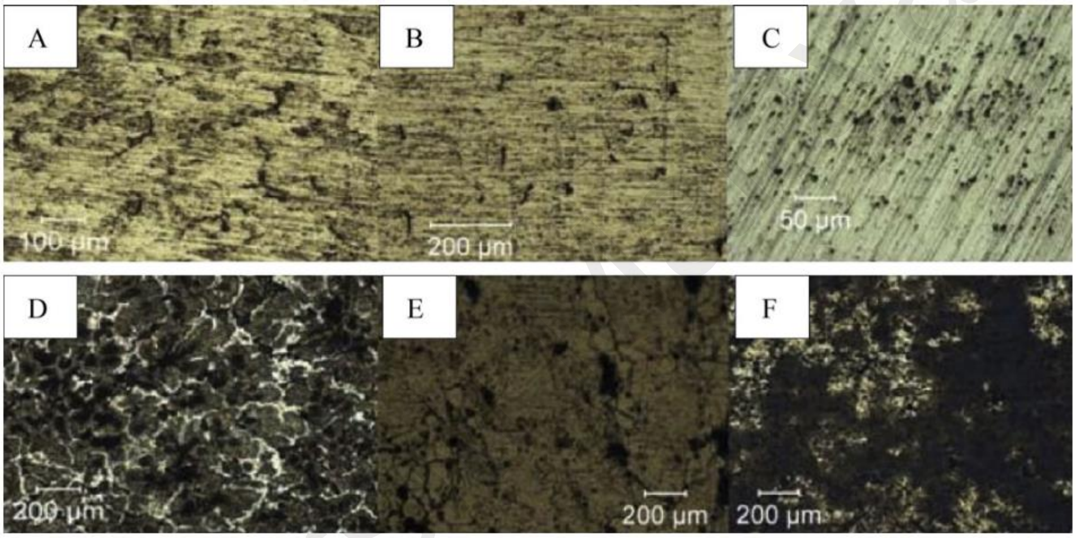

Figure 2.11: Reaction of specimens exposed in 0.1 NaCl with and without phosphate inhibitors. (Hill et al., 2011)

Last but not least, molybdates also one of the famous inorganic inhibitors. Molybdenum is an alloying element that is well-known for its ability to improve the passivation properties of stainless steels. Passivation is enhanced in steels of type 316 due to the presence of molybdenum as a minor element (Zaki Ahmad, 2006). At the iron anode of ferrous-ferric molybdenum oxide, sodium molybdate produces a complex passivation layer that protects the metal from corrosion. A study by Lopez-Garrity & Frankel (2014) concluded that a two-step method can lead to formation of molybdate whereby rapidly reduced to $\mathrm{MoO \cdot (OH)_2}$ over the intermetallic particles and is subsequently oxidized to intermediate molybdenum oxides in the presence of oxygen which satisfy the Zaki Ahmad (2006) statement where oxygen is required for the formation of the passive film to take place. The effectiveness of molybdates also been explore in prior studies by Moutarlier et al. (2003) described that the promotion of anodic layer formation and the improvement of corrosion resistance were both observed at high concentrations of the substance shown in Figure 2.11 below.

Table 2.4: The steady state voltage changes over time as a function of the molybdate content. (Moutarlier et al., 2003)

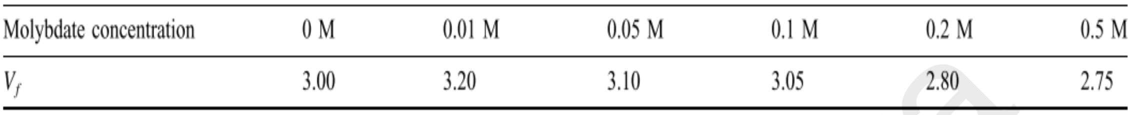

Molybdate concentration	0 M	0.01 M	0.05 M	0.1 M	0.2 M	0.5 M
V_f	3.00	3.20	3.10	3.05	2.80	2.75

A closer look on the result obtained by Moutarlier et al. (2003) shows the Vf values observed at doses ranging from 0.01 to 0.1 M are marginally higher than those obtained without the inhibitor. This shows that the development of films is not desirable. However, the concentrations of molybdate from 0.2 to 0.5 M, shows Vf value are lower emphasized that better film formation results as a result of these changes. The study of inorganic inhibitors are broad, therefore, additional studies to understand more completely on the inorganic inhibitors are required. In this case, only the most important and renown are explained.

2.5 General Corrosion Study

Corrosion is a capability of electrochemical processes to create a new compound that can lead to destructive of the surface of the material by oxidation (Hinds & Nimmo, 2015), electrolysis or chemical contamination which is dangerous and costly to the industry. Corrosion appeared to be one of the main contributors to the economic damages where “the global cost of corrosion to be $2.5 trillion annually” (NACE International, 2016). A consequence of having corrosion leads to oil pipelines break, chemical plant leak, the collapse of buildings and bridges, etc. These damages commonly affect metallic materials and generally produce oxide from the original metal which will generate the disintegration of surface metal. For instance, to illustrate the example of electrochemical corrosion is oxidation of iron atoms where the electrons are released at the anode and taken by cathode resulting in weakening the steel. Water serves as an electrolyte since the water exists almost 75% to 80% in the air. Hence, corrosion will not occur without the presence of water. Most of the metals tend to lose an electron when in the air or in water because they are easily oxidized, and as a result, corrosion occurs due to the exposure of the material. Nevertheless, corrosion also can be strongly affected by exposure of organic chemicals, bases, salts, and acids. There are various types of corrosion behaviour that can form on the surface based on the environment condition and these behaviours are shown in Figure 2.12 below.

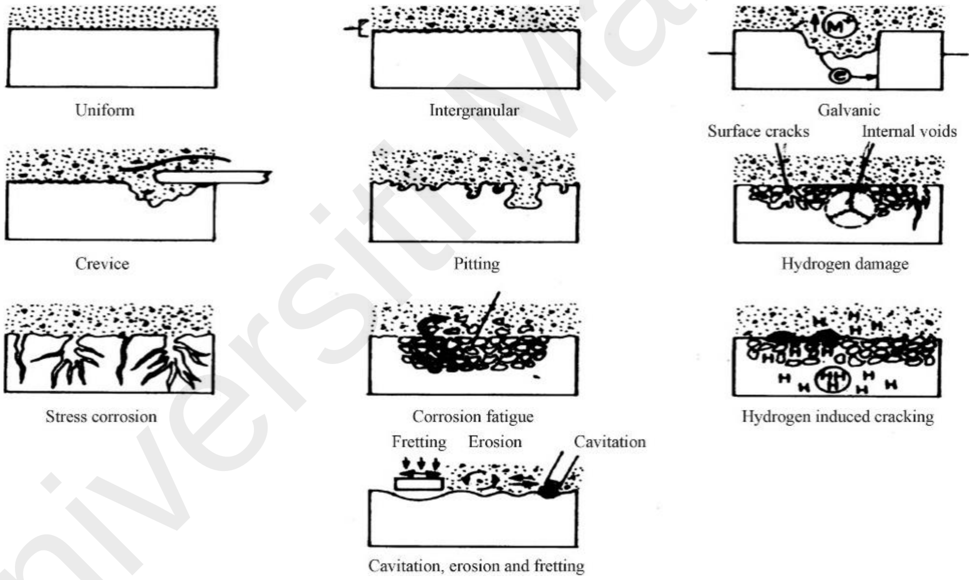

Figure 2.12: General types of corrosion. (Chaturvedi, 2009)

Corrosion can occur in all metals, but some metals acquire a natural passivity that is capable to form its natural protection when reacts with oxygen in the air. This natural passivity is the formation of thin oxide film and prevents the metal from performing further reaction (Escobar & Cantu, 2007).

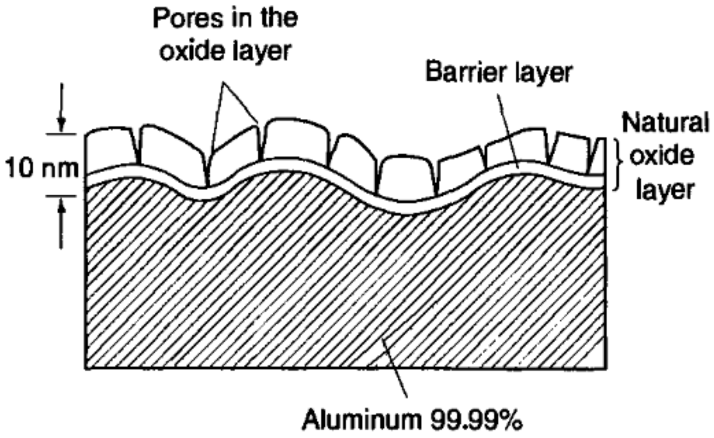

Figure 2.13: Formation of thin oxide film on pure aluminium. (Davis, 1999b)

The oxide film that forms in typical atmospheres consists of two layers (Baboian et al., 2005), as shown in Figure 2.13. The inner oxide layer, which is closest to the metal, is a compact amorphous barrier layer whose thickness is completely governed by the ambient temperature. The limiting barrier thickness in oxygen, dry air, and wet air is the same across any temperature. A thicker, more permeable outer layer of hydrated oxide protects the barrier layer. The chemical properties of the oxide layers that surround the metal, whether at low or high temperatures, have provided the foundation for understanding aluminium corrosion processes. One way to think about the natural film is as the product of a dynamic equilibrium between opposing forces, in which attempting to construct the compact barrier layer and attempting to destabilise it. Natural film is only composed of the barrier layer when aggressive ions are absent, such as in dry air, the, however, if protection fails, metal will corrode due to damage of the thin film. The Pourbaix plot in Figure 2.14 below depicts the conditions for thermodynamic stability of the oxide film explained by Davis (1999b). In the pH range between 4 to 8.5, aluminium is protected by its oxide film and is considered to be in a passive mode. The range's boundaries, on the other hand, fluctuate depending on the type of oxide film present, temperature, and the presence of chemicals that can form soluble complexes or insoluble salts with aluminium.

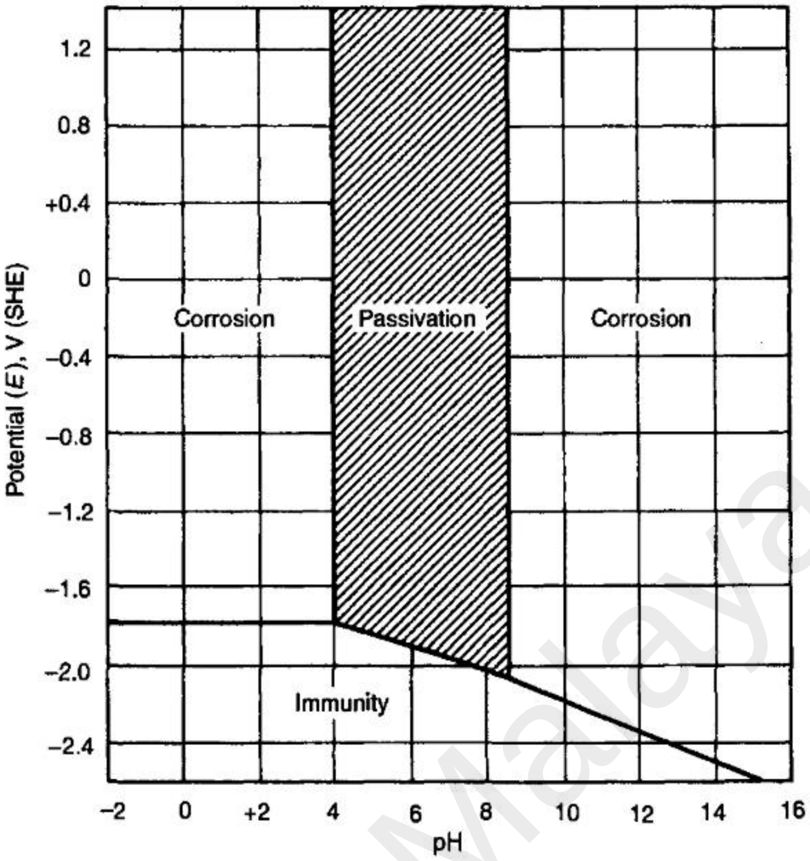

Figure 2.14: Pourbaix diagram of Aluminium under several conditions. (Davis, 1999b)

In some cases, the oxide film usually re-passivates but it depends on the environment. In this case, corrosion behaviour of 5xxx series of aluminium alloys usually suffers from intergranular corrosion cracking (ICC) and stress corrosion cracking (SCC)(Braun, 1998) which will be justified on the next section.

2.6 Corrosion Behaviour of 5xxx series Aluminium Alloys

It is known for its non-heat treatable, superior corrosion resistance, which makes the 5xxxx series of aluminium alloy a popular choice for industrial applications. However, the industrial sector has a high concern about the downside of this material, the 5xxx series (Al-Mg-based) aluminium alloys are susceptible to intergranular corrosion (IGC) and intergranular stress corrosion cracking (SCC) when subjected to temperatures ranging from 50 °C to 200°C over an extended length of time. As mentioned in section 2.2.2, this effect is also referred to as sensitization and a phenomenon which is generally connected with the selective dissolution of beta phase (Al3Mg2), which precipitates on grain boundaries when being exposed to high temperatures (Davenport et al., 2006; Searles et al., 2002). In service, the alloys become more sensitive to intergranular corrosion cracking (IGC), and the rate of sensitisation rises with increasing magnesium (Mg) content as well as with preceding plastic deformation of the alloys in service. When these alloys are used in industrial applications, they have a limited lifespan, especially if they are subjected to high temperatures during their operational lifecycle. The formation of an SCC-susceptible microstructure must be defined to prevent the development of stress corrosion cracking (SCC).

Figure 2.15 is adapted from Cormack (2012) and it shows a graphic of the stress corrosion cracking (SCC) process. Stress corrosion cracking (SCC) requires a corrosive environment and some external forces to occur (Golumbfskie et al., 2016).

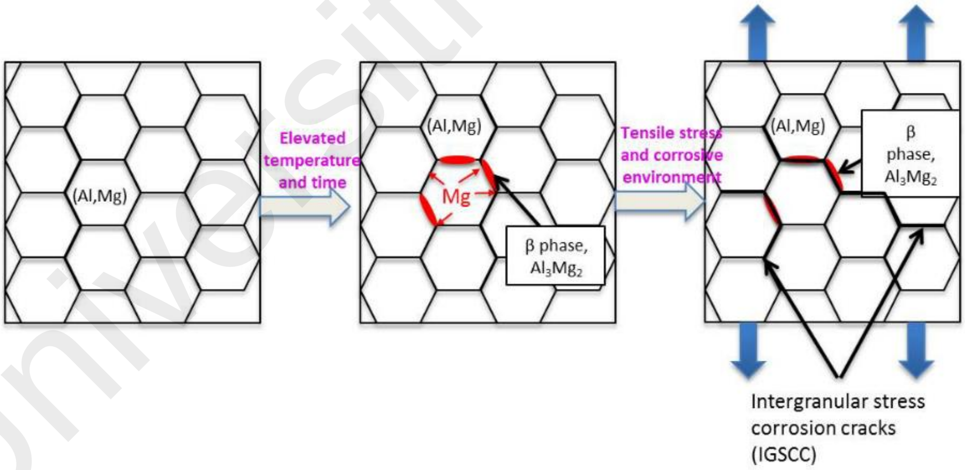

Figure 2.15 Process of Intergranular Stress Corrosion Cracking (IGSCC) in Al-Mg during sensitization. (Cormack, 2012)

The diagram depicts the progression of SCC in an Al-Mg alloy. When a material is exposed to a high temperature for an extended period of time, sensitization β phase Al_3Mg_2 develops at the grain boundaries, as shown in the centre image. The dissolution of the β phase precipitates happens when a tensile load is applied in a corrosive surroundings, resulting in the formation of intergranular stress corrosion cracking. It was documented by Golumbfskie et al. (2016) when the material was subjected to further stress, the cracks began to link and expand along the grain boundary networks, and the material eventually broke. Failure occurred in the material was mechanically assisted corrosion (Roberge, 2000), permitted the indication to be attained at a faster rate. As mentioned in the Roberge (2000) handbook, the contribution of crack growth is not only from applied stresses, but the formation of stress corrosion cracking (SCC) also has additional stress contributions caused by corrosion as compared to fatigue crack. As demonstrated in Figure 2.16, there were several cases of fracture formation that were caused by stress corrosion cracking (SCC) in the Golumbfskie et al. (2016) literature.

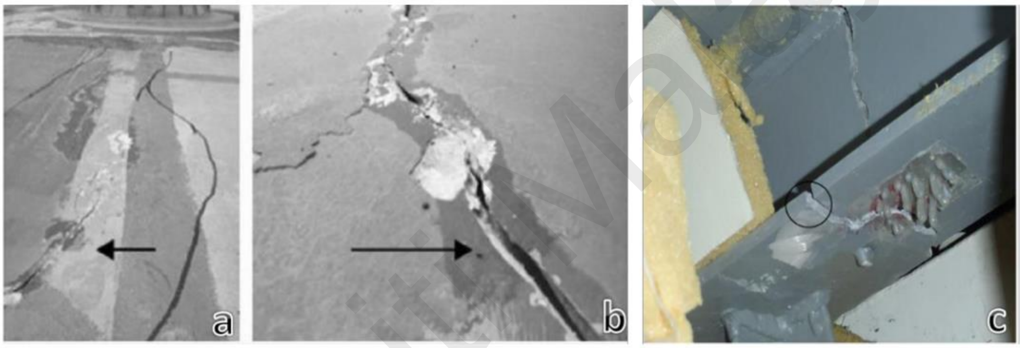

Figure 2.16: Example of stress corrosion cracking (SCC) caused by β phase corrosion in 5xxx series of aluminium alloy.(Golumbfskie et al., 2016)

These photographs clearly show how sensitization and subsequent SCC can cause severe damage. As a result, numerous studies have been performed to achieve a of better understanding of the process and causes of SCC in alloys of the 5xxx series. According to the findings by Searles et al., greater β phase levels are affected from low ductility and mechanical properties. Davenport et al. (2006) also observed the spreading of intergranular corrosion (IGC) and stress corrosion cracking (SCC) of sensitised 5xxx series of aluminium alloys. When aluminium with 4.5 wt% of magnesium (Mg) content is exposed to a certain service temperature for an extended period of time, it may become prone to intergranular corrosion (IGC) due to the precipitation of Mg-rich β-phase at grain boundaries, which may result in stress corrosion cracking (SCC). The susceptibility of 5xxx series of aluminium alloy to the defect was shown to be highly dependent on the heat treatments used to sensitise the compound (Davenport et al., 2006).

2.7 Corrosion Analysis

Corrosion analysis is generally conducted in laboratories to mitigate the issues regarding corrosion. Commonly, infrastructure products and industrial materials are often put under tests for failure study before proceeding to the next stage. All corrosion tests are created by expert failure analysts such as engineers and chemists. Conducting corrosion test will contribute to making the right decision in the selection of material, processing, and treatments.

There are a few types of corrosion test can be conducted in a laboratory. Expert analyst often focused on these four tests, which are electrochemical measurement, immersion, heat transfer and corrosivity. The industry is concerned about the quality standard of every product, therefore, testing the materials is required. Overall, the most popular and basic type of corrosion test is electrochemical corrosion test and salt spray chamber test.

Electrochemical corrosion test involves the immersion of the test sample for a couple of hours to determine the corrosion rate. The data generally are obtained from a potentiostat machine. All the information related to the sample is plotted in a graph called potentiodynamic polarization curves. Thus, Tafel extrapolation method is used to attain the value such as potential corrosion and current density corrosion from the anodic and cathodic intercept.

2.7.1 Potentiodynamic Polarization Curves

Monitoring the resultant current flow and changing the potential both involve in potentiodynamic polarization technique as this technique principally is used to determine the corrosion tests. All information of the sample can be obtained from the technique such as determining the corrosion rate, sample passivation, and type of corrosion that affect the sample after the immersion test has been completed.

The data achieved from the potentiodynamic polarization scan determine all the information as a curve graph shown in Figure 2.17. The regions on the graph define the behaviour of the sample as the scan starts from the cathodic region at point A, and progressively increases in potential until it reaches point F, then terminates.

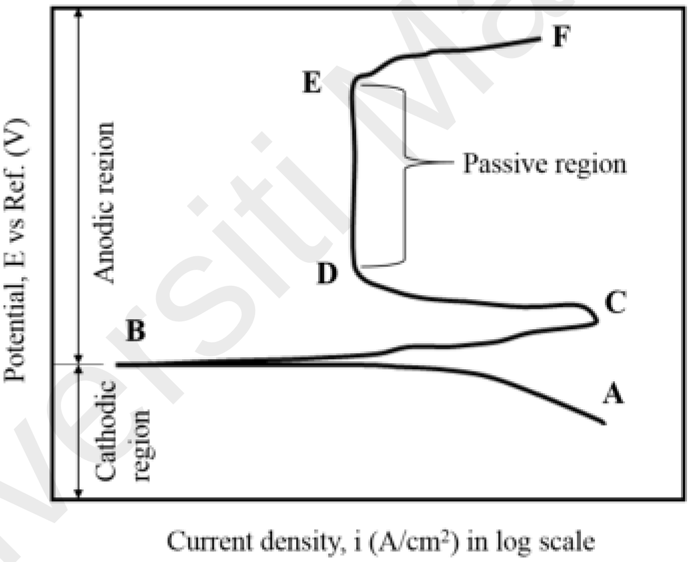

Figure 2.17: An example of potentiodynamic polarization curves data.

Current density (A/cm^2) represents the y-axis in the log scale, meanwhile, potential (V_{SCE}) represents the x-axis. Aforementioned, the curve starts at point A. As the curve reaches at point B where the corrosion potential (E_{corr})is located, the summation of anodic and cathodic reaction rates towards electrode surface is zero. The current density increases rapidly from point B towards point C as the potential increases which explains the active region of metal oxidation.

The curve continues to plot from point C towards point D where it can be observed that the increase of potential lead to the decrease of current density. It is termed as passivation potential (E_{pass}). The decrease of current density will last until it reaches point D when the low passive current density is achieved. A long straight line upward occurred at DE region where the current density (A/cm^2) is almost constant with the potential, forming a passive region. The current density again accelerates toward point F which is the factor due to trans-passive dissolution.

2.7.2 Tafel Extrapolation

Tafel extrapolation is a polarization technique that is used to measure the corrosion rate. Compared to the weight loss estimation experiment, the polarization method produces a much quicker result. The curves display linear behaviour in the potential (E) versus current density (A/cm^2) graph called tafel behaviour. Classic example of polarization behaviour is shown in Figure 2.18 below in which it demonstrates the presence and absence of oxygen produced from metal placed in an acidic environment.

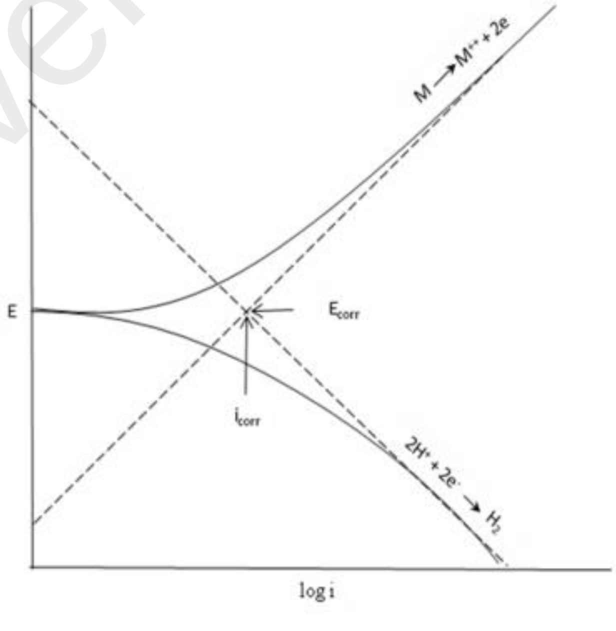

Figure 2.18: Potentiodynamic polarization curves data of metal in an acidic environment.

The dashed line of intersection point in Figure 2.18 refers to extrapolation of anodic and cathodic Tafel slopes and corrosion rate. Therefore, the value of corrosion potential (E_{corr}) and corrosion current density (i_{corr}) can be obtained achieved directly from cross-over point. Anodic branch and cathodic branch represent the chemical reaction equation 2.3 and 2.4 as follows.

- $M = M^{++} + 2e$ for anodic branch (2.3)
- $2H^{+} + 2e = H_2$ for cathodic branch (2.4)

Tafel constant is interpreted from the slopes of cathodic and anodic - (β_a and β_c) as shown in Figure 2.19 below.

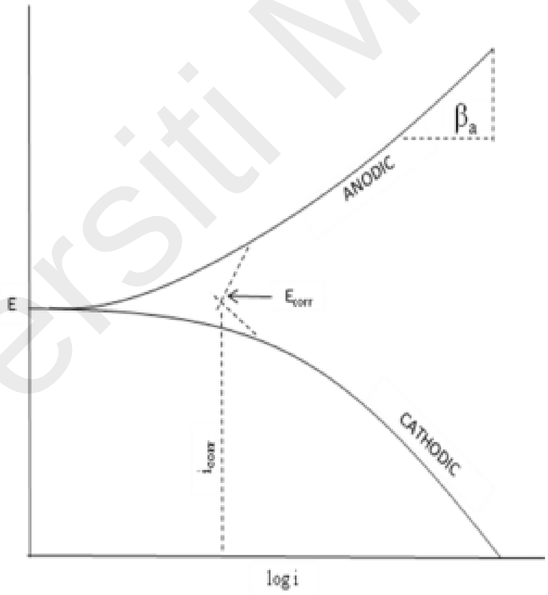

Figure 2.19: Tafel constant from the anodic and cathodic branch.

Tafel method provides a good accuracy in observing the corrosion rate but, the deficiency of Tafel extrapolation becomes tougher to achieve in accuracy when ohmic resistance and concentration polarization is taking over. To attain a good result, it is compulsory to obtain the steady-state polarization curves to ensure more representative of corrosion reactions.

There are some shortcomings in Tafel extrapolation due to effect from environmental condition and experimental. Also, the polarization curve is not reversible, therefore, Tafel constant can differ. Generally, the polarization curve is affected where anodic curves may not exhibit linear behaviour near potential corrosion (E_{corr}).

2.7.3 Scanning Electron Microscopy (SEM) / Energy-Dispersive X-ray Spectroscopy (EDS)

Scanning electron microscopy is a method for high-resolution imaging of sample surface and objects using a scanning electron microscope. The SEM is commonly equipped with energy dispersive X-ray spectroscopy (EDX). In the SEM high energy beam of electrons is directed on the specimen from an electron gun under vacuum. An interaction occurs between the electrons and the atoms of the sample. The sample emits x-rays, backscattered electrons and secondary electrons which are collected by the detector. Qualitative chemical analysis of particular points can be done with EDX operations as the X-rays is a characteristic of the element from where it is emitted. Therefore, chemical components of a sample can be identified with EDX. SEM has the following components mainly,

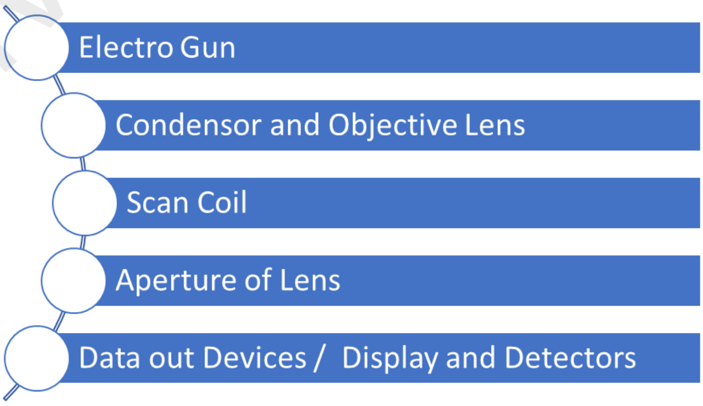

Figure 2.20: List of components required for Scanning Electron Microscopy (SEM).

In the present study, the morphology of the Al-Mg was studied using SEM before and after electrochemical corrosion measurements. Furthermore, in order to study the elemental composition of the solder alloys and the corrosion products, SEM/EDX microscope was used.

2.7.4 Optical Microscopy

Optical microscopy can be described as the foundational tool for material characterisation in advanced scientific study. Despite its reputation as a basic tool, it is capable in providing extremely precise information regarding material preparations, heat treatment prior to observation, material flaws, and alloy composition. Optical microscopy will likely serve as a useful tool in science for a long time. Soft material such as aluminium, tin, etc, easily affected by deep scratch lines, imbedded abrasive particles, dust particles, and water stains covering the polished surface all provide substantial obstacles during their preparation. Microscopy may at times include all or some of the procedures listed in Figure 2.21 below. Although the first phases of specimen preparation are often overlooked, they are the most vital if accurate, factual, and conclusive evaluations are to be obtained.

Figure 2.21: List of procedure required for Optical Microscopy test.

To summarise, in most research studies, an exceptional quality optical microscope and microscopy as a technology will continue to play a crucial role during decision making, and a polished surface will only provide correct information on a given specimen if all preparation stages and steps are considered, followed, and carried out on the specimen properly and professionally.

2.8 Summary and Conclusions

The 5xxx series of aluminium alloy has an excellent corrosion resistance but can never withstand a in a high corrosive medium. If Al-Mg subjected to a temperature >50 degree, the stress corrosion cracking (SCC) and intergranular corrosion cracking (IGC) will appear right after the formation of β equilibrium phase. Previous research appears to validate the view that inorganic inhibitors showed better corrosion resistance among the alloys, however, the efficacy of the inhibitors depends on the type of materials. Results revealed that the corrosion resistance is largely dependent on the concentration of inhibitor, more concentration content resulted larger passivation range. Among the range of inorganic inhibitor, each of them has their pros and cons. Thereupon, the result and discussion section will provide the whole overview of the inorganic inhibitor on the 5xxx series of aluminium alloy.

CHAPTER 3: METHODOLOGY

3.1 Sample preparation

Table 3.1 represents the chemical composition of investigated steel. In this experiment reviewed, 5xxx series of aluminium alloys were used. The table below shows the percentage composition of all designation of Aluminium (Al-Mg) with other alloying elements. The 5xxx series of Aluminium Alloy steel composition consists of Magnesium (Mg), Silicon (Sn), Iron (Fe), Manganese (Mn), Chromium (Cr), Copper (Cu), Zinc (Zn) and other micro-alloying elements. The manufacturing process that was used to obtain this composite metal was casting method where both metals were heated to liquid form and mixed into a mould to attain a desired shape (Constantin et al., 2008; M. A. Deyab et al., 2017; Liu et al., 2016; Wang et al., 2021; Zhu et al., 2019).

Table 3.1 : Composition of 5xxx series of Aluminium alloy research sample. (Constantin et al., 2008; M. A. Deyab et al., 2017; Liu et al., 2016; Wang et al., 2021; Zhu et al., 2019)

Elements	Al%	Mg%	Si%	Fe%	Mn%	Cr%	Cu%	Zn%
A5052	94.75	2.2	0.25	0.3	0.1	0.1	0.1	0.1
A5754	96.1	2.6	0.4	0.4	0.5	-	-	-
A5058	92.45	5.0	0.4	0.4	1.0	0.25	0.1	0.25

The experimental design employed from the reviewed article was electrochemical corrosion analysis. Prior to each experiment, the required apparatus to conduct this experiment were a potentiostat, which was used to record the electrochemical corrosion data, a beaker that was able to hold the electrodes and the electrolyte. In this experiment, the authors introduced three different electrodes to be considered in this case such as reference electrode (saturated calomel, SCE), the counter electrode (platinum wire) and the working electrode (test sample) as well as working electrode holder.

Based on the sample prepared by the authors, a sufficient surface area required to prepare the sample use in electrochemical measurement and weight loss for this experiment. The sample was shaped into a cube and inserted into a cylinder tube. Once the cube was placed properly, epoxy resin was poured into the cylinder tubing and left only the top surface of the specimen to be exposed. The test sample was left for overnight for epoxy resins to completely harden. The process can be referred graphically in Figure 3.1 below.

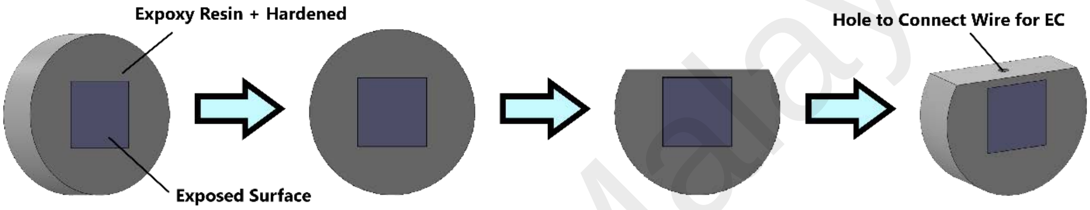

Figure 3.1: Sample preparation for the research.

The process continue with the top surface of the sample was then abraded using Grinder-Polisher machine with different grades of emery papers from coarse to very fine at 280 rpm. According to the authors, the completion of the abraded process is then scrubbed with the household detergent and rinsed thoroughly with tap water and left to dry for a couple of minutes. Next, the diamond compound paste was applied onto the surface of the sample and then the sample's surface was polished using polisher at 300 rpm. Once the sample microstructure met the requirement, the surface was then cleaned with the alcohol to remove the potential contamination.

For a sample to be connected to the potentiostat, a wire with a screw must be attached to the specimen. As shown in Figure 3.1 above, the sample was cut on one side and a blind hole was created until it reached the steel. The blind hole was then threaded with a drill manually for screw to be attached. The electrochemical corrosion test in a standard compartment cell shown in the full schematic Figure 3.2 below. The configuration of a cell operates with three different electrodes in potentiostat.

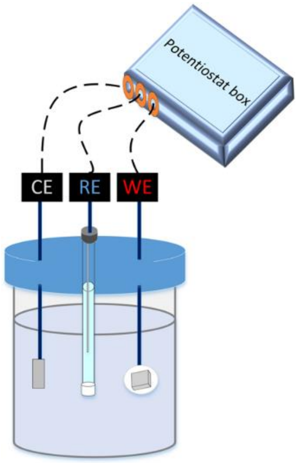

Figure 3.2: Experimental setup for this research.

The beaker containing corrosive solution with concentration which acted as an electrolyte for this experiment. All three electrodes were placed in the beaker and the steel sample was fully immersed leaving only the working electrode cable above the solution. Before conducting the experiment, the potentiostat had to be calibrated according to experimental measurement to avoid false results. The experiment was carried out in room temperature of 25 degree (Constantin et al., 2008; M. A. Deyab et al., 2017; Liu et al., 2016; Wang et al., 2021; Zhu et al., 2019).

3.2 Preparation of corrosive and inhibitive solution

One of the most important abilities at all levels of chemistry related experiment is to prepare of a solution of a specific concentration. In the case of solutions preparation, it is express the amount as a concentration which refer as Molarity (M). Before beginning, the authors map out the procedure for preparing the corrosive solution. As an example, on equation 3.1, the experiment required to prepare 0.25 molar solution which represent:

$$0.25\ \mathrm{M} = \frac{0.25\ \mathrm{mol}}{1\mathrm{L}} \tag{3.1}$$

An example again where this experiment only required 0.5 L of this solution, thus multiply the above terms together will determine the amount of moles concentration needed for this experiment.

$$0.5\ \mathrm{L} \times \frac{0.25\ \mathrm{mol}}{1\mathrm{L}} = 0.125\ \mathrm{mol\ (acidic)} \qquad (3.2)$$

Specifically, to determine the exact mass the value of 0.125 mol is multiply with the mass (xxxx) of the solid (g/L) which given example below:

$$0.125\ \mathrm{mol} \times \mathrm{xxxx}\frac{\mathrm{g}}{\mathrm{mol}} = \mathrm{xxxx\ g\ (acid\ solid)} \qquad (3.3)$$

Hence, the amount required for solid acidic is determined. First of all, scoop an amount of acidic solid and using a weighing scale to attain a desire mass calculated using the formula above. Once the solid measured, transfer all the solid into an appropriate size of a volumetric flask. Next add enough amount of water into the volumetric flask to an approximately half full which giving enough space to stir the solid to a complete dissolved. Important to know that is critical that all solid is dissolved prior to filling to the appropriate volume as different solutes may take up more volume in solution than their undissolved salts. Once the solid is fully dissolved, the volumetric flask is filled with water up to the mark. The process can be illustrated in Figure 3.3 below.

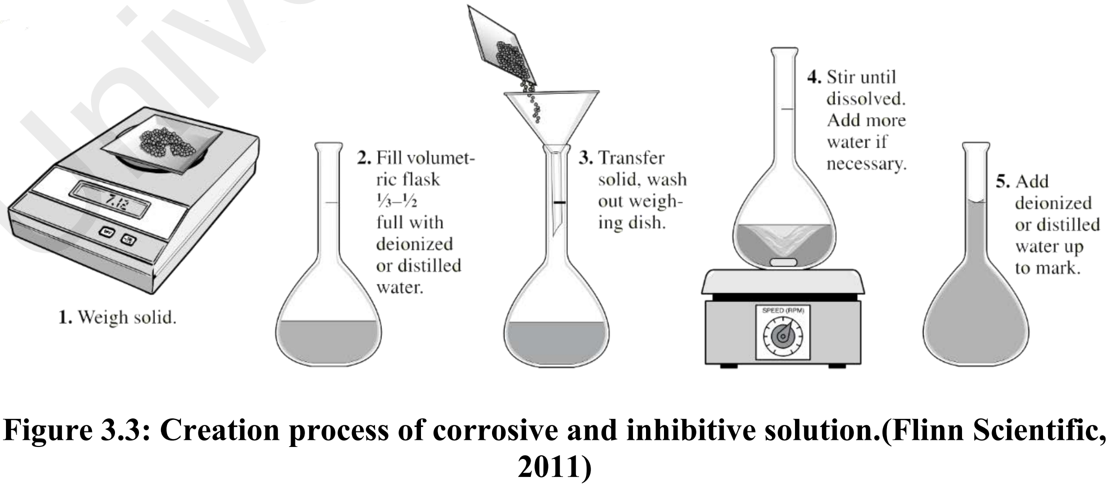

Figure 3.3: Creation process of corrosive and inhibitive solution.(Flinn Scientific, 2011)

3.3 Experimental Procedure

As per assessed from the Constantin et al. (2008), M. A. Deyab et al. (2017), Liu et al. (2016), Wang et al. (2021), Zhu et al. (2019) experimental procedure, polarization measurement was carried out once the sample was connected to a potentiostat and the sample was immersed into the corrosive solution. To lessen the severity of corrosion, inhibitors are usually applied in small amounts to acids, cooling waters, steam, and a variety of other conditions, either constantly or occasionally. In this case, the authors applied a small amount of inhibitors solution combined with acids and left to soak to several hours and days. In the literature of Wang et al. (2021), the inhibitors solution mixed with natural seawaters. The authors set the experiment to a certain scan rate using saturated calomel (SCE) and platinum wire as the reference electrode and the counter electrode. In the reviewed article, the sample was left immersed in the solution for several hours and days, and all the electrochemical measurement would be attained from the software. The sample is then undergoing scanning electron microscopy (SEM) and energy dispersive X-ray spectroscopy (EDX). The data from the articles can be seen on the result and discussion below.

CHAPTER 4: RESULT & DISCUSSION

4.1 Introduction

In this chapter, the result of electrochemical corrosion measurement and characterization of 5xxx series of aluminium alloy (Al-Mg) has been analysed and discussed in detail through previous studies. Consequently, this chapter has been classified into several subcategories according to the types of inorganic inhibitor.

The results obtained in this project are categorised into three parts. The first part presents the results obtained from electrochemical corrosion analysis such as potentiodynamic polarization test. The second part deals with the characterization of the corrosion react with or without inorganic inhibitors which include morphological and compositional analysis.

4.2 Electrochemical corrosion analysis

This section presents the results obtained from the potentiodynamic polarization test on 5xxx series of aluminium alloy with different types of inorganic inhibitors.

4.2.1 Potentiodynamic polarization results

The potentiodynamic polarization test was performed for all 5xxx series of aluminium alloy (Al-Mg). Following the completion of the test, a variety of plots was acquired and subsequently examined. By using the software, the corrosion parameters were obtained via Tafel plot. The polarization studies provide interpretation of the corrosion behaviour of the corresponding 5xxx series of aluminium alloy (Al-Mg).

4.2.1.1 AA5754 containing chromate or molybdate

The results in Figure 4.1 demonstrated in this chapter match state of the art of polarization curves which represent the potentiodynamic polarization curves for AA5754 containing chromate or molybdate as an inhibitor. The test was polarized for up to +0.242V with a voltage scan rate of 0.166 mV/s, in eutectic solutions contain Ammonia Chloride (NH4Cl) about 12-13wt% and Sodium Nitrate (NaNO3) about 27-28wt%. The corresponding polarization parameters such as corrosion potential (E_{corr}) and corrosion current (i_{corr}) values were obtained from the polarization curves are plotted in Figure 4.1. The result showed that the critical current density for molybdate inhibitor is comparatively higher than that of chromate inhibitor.

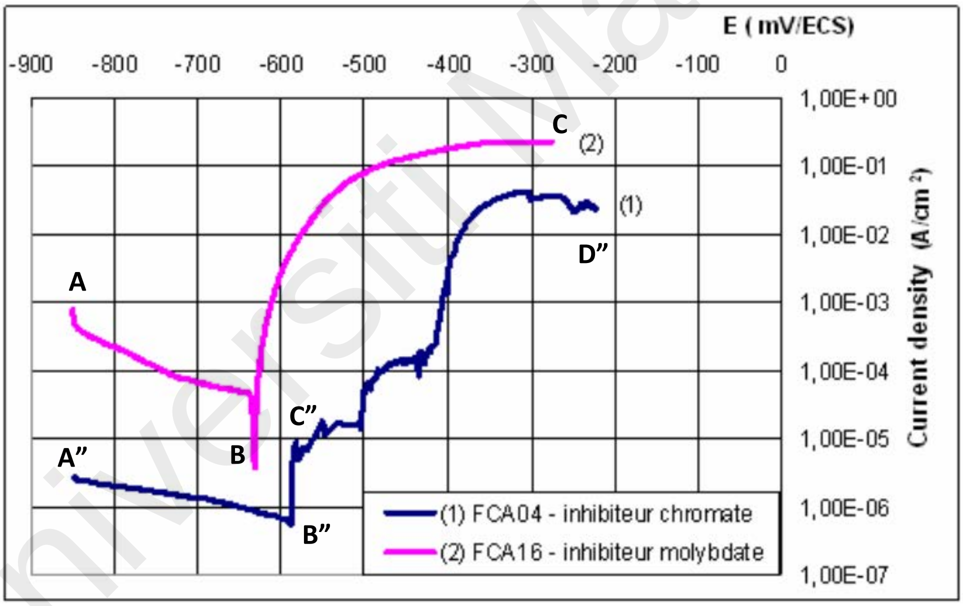

Figure 4.1: Potentiodynamic polarisation curves for AA5754 inhibited by chromate or molybdate in eutectic solutions containing NH4Cl (approx. 12-13wt%) and NaNO3 (approx. 27-28wt%). (Constantin et al., 2008)

In this study by Constantin et al. (2008), all the corrosion tests were performed in eutectic solution contain Ammonia Chloride (NH4Cl) about 12-13wt% and Sodium Nitrate (NaNO3) about 27-28wt%. The values of free potential obtained are similar, as shown in Table 4.1 describes the stability value is around -650 mV/SCE for test featuring chromate or molybdate in eutectic solution.

Table 4.1: Free potential and corrosion current density of AA5754 in chromates or molybdates.(Constantin et al., 2008)

Metals	Solutions			
	With chromate		With molybdate	
	E(mV/SCE)	I (μA/cm^2)	E(mV/SCE)	I (μA/cm^2)
Al plate	-650	1.3-1.4	-650	51-52

A novel finding in Constantin et al. (2008) literature from Table 4.1 shows the corrosion potential values calculated from the potentiodynamic polarisation curves. Together, the findings confirmed that both examples have the same magnitude, nevertheless, in the molybdate-inhibited solution, the aluminium alloy is a little less noble which explains the less noble metal has a lower electrode potential than the nobler metal, and as a result, it will serve as the anode in the electrolyte device. In the presence of chromate inhibitor, it is noticed that an anodic passivation plateau occurs (Constantin et al., 2008). In this case, the plateau refers to the time required for the creation of protective films. It is approximately 50 times smaller than the values of current density ($\mu A/cm^2$) in the molybdate solution when using chromate as a solvent.

As explained in the corrosion analysis of potentiodynamic polarization curve in Figure 2, region of AB/A"B" in Figure corresponds to the cathodic reduction reaction where it elucidates the dissolved oxygen reduction reaction before it reaches at B/B" where the summation of anodic and cathodic reaction rates towards electrode surface is zero. Both curves started at the same potential at a value of -650 mV/SCE but the value of corrosion current density differs. The curve behaviour inhibited by molybdates shows the increase in anodic sharply increased the current density. This linear region corresponds to the dissolution of active materials. This reaction also suggested the formation of a thin passive film from the molybdates that enhance the corrosion resistance. However, the curve behaviour for chromates seems to have disturbance. It was suspected that the disturbance can occur due to the experimental error. Major drawbacks in this literature since the explanation is insufficient, thus, failed to provide an adequate proof on the curve behaviour occurred in chromate inhibitor.

The analysis has not met with the purposed of this review as raises several doubts especially on how the concentration of molybdates and chromates will affect the inhibition efficiency under corrosive. Nonetheless, the findings demonstrates that chromates and molybdates able to gives a protection from the corrosion.

4.2.1.2 AA5052 and AA5754 containing sodium molybdate

The above findings in line with the ideas of Deyab et al. (2017) where the author employed an almost identical literature. In 2017, Deyab and his team in prior studies examine the trend of corrosion and corrosion inhibition in aluminium alloy of A5052 and A5754 series. However, this literature differs in that it uses sulphuric acid (H_2SO_4) as a corrosive medium. In particular, the inorganic inhibitors used in this studies by Deyab et al. (2017) is sodium molybdate ($Na_2MO_2^{-4}$) and aluminium alloy of A5754 series where this section review the literature almost related to Constantin et al. (2008). These results of literature studied by Deyab et al. (2017) go further where the sodium inhibitors ($Na_2MO_2^{-4}$) is compared with sodium tungstate ($Na_2WO_2^{-4}$) on its efficacy towards protecting the aluminium alloy from corrosion. The study of this comparison with sodium tungstate ($Na_2WO_2^{-4}$) will not be addressed in this chapter.

Studies of sodium molybdate ($Na_2MO_2^{-4}$) as an inhibitor are well documented, it is also acknowledged by Deyab et al. (2017) that aluminium alloys of A5052 and A5754 are less corroded when MO_2^{-4} anions are presence in the acid solution. In short, the chemical composition of A5052 and A5754 shows in Table 4.2. The measurements were carried out by automatically adjusting the electrode potential from 0.25 to + 0.25 V (SCE) with respect to OCP at a scan rate of 1.0 mV/s. A5052 and A5754 electrode surfaces were evaluated after the necessary tests were carried out using a scanning electron microscope to determine the elements that were present on the electrode surface, which will be addressed in more detail hereafter.

Table 4.2: Chemical composition of A5052 and A5754. (M. A. Deyab et al., 2017)

Elements	Al%	Mg%	Si%	Fe%	Mn%	Cr%	Cu%	Zn%
A5052	94.75	2.2	0.25	0.3	0.1	0.1	0.1	0.1
A5754	96.1	2.6	0.4	0.4	0.5	-	-	-

Deyab et al. (2017) have emphasized the necessity of research in which investigations are conducted with and without sodium molybdate ($Na_2MO_2^{-4}$) in (H_2SO_4) to investigate the efficacy of the inhibitor. Using the potentiodynamic polarisation method, the effect of ($Na_2MO_2^{-4}$) inorganic salts on the two aluminium alloys A5052 and A5754 in aerated and stagnant H_2SO_4 acid solution was examined. Polarisation curves of aluminium alloy A5052 in $0.3\ M\ H_2SO_4$ in the absence and presence of various concentrations of molybdate anions are shown in Figure 4.2 with parameters of $1.0\ mVs^{-1}$ and $298\ K$. E_{corr} and I_{corr}, two electrochemical kinetic parameters, were also determined and are reported in Table 4.3. However, the polarization curves of aluminium alloy in A5754 are not recorded in the literature apart from the data listed on Table 4.3. The results of the experiment promising finding where presence of sodium molybdate in the corrosive media lowers the corrosion current density (I_{corr}), showing that these oxyanions protect the alloys from corrosion attack. Together, the present findings of confirm with higher concentrations sodium molybdate, this oxyanion inhibitory properties improve. Furthermore, the existence of this inhibitors affecting the corrosion potential (E_{corr}) of the alloys to be shifted to less negative values, demonstrating that these oxyanions serve as anodic type inhibitors (M. A. M. Deyab, 2015; Hayyan et al., 2012). Deyab et al. (2017) express that the ability of these anions to inhibit depends on their kind and concentration.

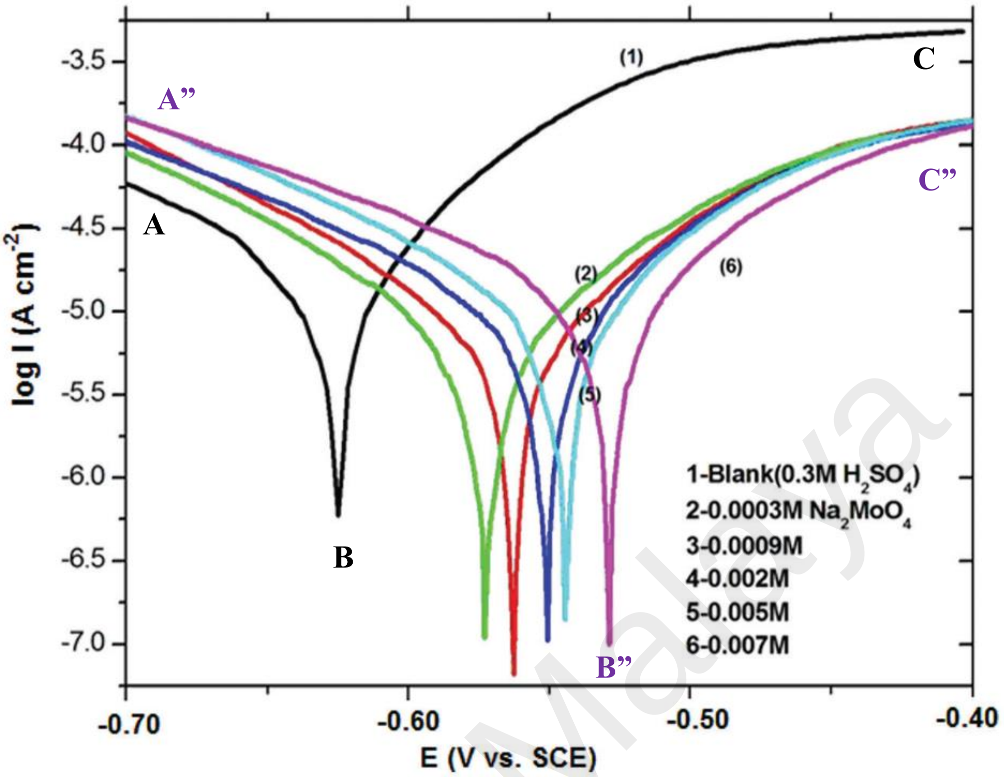

Figure 4.2: Polarization curves of A5052 in $0.3\ M\ H_2SO_4$ with different solution and concentration of sodium molybdate. (M. A. Deyab et al., 2017)

Additional studies to understand more completely the key tenets of the polarization curves by explaining the behaviour curves in depth. The behaviour of the polarization curves of AA5052 alloy in 0.3 M H_2SO_4 (blank) and 0.3 M H_2SO_4 + 0.007 M molybdate inhibitor is studied. Region AB/A"B" in Figure 4.2 resembles the cathodic reduction reaction. As the tests were performed in 0.3 M H_2SO_4 solution, the authors define that the reduction reaction occurring can be described to the dissolved of oxygen reduction reaction shown in equation 4.1 below,

$$O_2 + 2H_2O + 4e^- \rightarrow 4OH^- \qquad (4.1)$$

The corrosion potential (E corr) is the potential at point B and B" where the extrapolated anodic and cathodic Tafel slopes intersect, and the current becomes zero. The dissolution of AA5052 begin with the increasing potential from point A to point B. Starting from polarization curve at B (AA5052 alloy in blank solution of 0.3 M H_2SO_4), a shift in the corrosion potential ($\mathrm{E_{corr}}$) towards negative values indicating the dissolution being started at lower potential. The point B is then continuing its progress toward points C where it indicates the formation of natural passivation film. However, the natural passivation film did not last longer as the current density shifted more towards positive value and the curves ends approximately more than -3.5 A $\mathrm{cm^2}$ which demonstrates the limitation of passive film to protect the surface alloy from aggressive ions. As for polarization curve at A" (AA5052 alloy in blank solution of 0.3 M $\mathrm{H_2SO_4}$ with 0.007 M molybdate), a shift in the corrosion potential ($\mathrm{E_{corr}}$) towards higher values compared to blank solution indicating the dissolution being started at higher potential. At the end of the cathodic polarization at point B", the increase in anodic sharply increased the current density. This linear region corresponds to the dissolution of active materials. This reaction also suggested the formation of a thin passive film from the molybdates that enhance the corrosion resistance. To compare, the value of current density at blank solution is more than the one with inhibited by molybdates at an approximate of -4.0 A $\mathrm{cm^2}$. Thus, molybdate proved to gives a better protection on the AA5052 alloy. No trans-passive dissolution was found in the polarization curve shown in Figure 4.2.

Although results appear consistent with showing the efficiency of the inhibitor, the literature appear inconsistent in presenting the result. Therefore, important issue in the literature review where the behaviour of polarization curves for A5754 is not presented, thus, limiting the debate on comparing the literature on Constantin et al. (2008).

From Table 4.3, the value of the inhibition efficiency of sodium molybdenum ($Na_2MO_2^{-4}$) added into the (H_2SO_4) solution was calculated using the equation 4.2 below depicted from (Godínez et al., 2003; Handbook, 2015; Ivušić et al., 2000; Uma et al., 2016).

$$\eta_p\% = \frac{I_{corr}^o - I_{corr}}{I_{corr}^o} \times 100 \tag{4.2}$$

As mentioned earlier, the effectiveness of inorganic inhibitors rises as their concentration is increased which corresponds to the findings. The adsorption of MO_2^{-4} oxyanions on the surfaces of alloys is thought to be responsible for their inhibitory properties. The adsorption of oxyanions on the surface of an alloy prevents the active sites accessible for corrosion processes from being available. In acid solutions, a rise in inhibitor concentration leads to an increase in surface covering, which increases the effectiveness of the inhibitor as a protector (M. A. M. Deyab, 2015).

Table 4.3: Inhibition efficiency and electrochemical parameters for A5052 and A5754 alloys with or without $Na_2MO_2^{-4}$ inhibitors at 0.3 M H_2SO_4 at 298 K.

$\mathbf{Na_2MO_2^{-4}}$ (M)	$\mathbf{I_{corr}}$ ($\mathbf{\mu A\ cm^{-2}}$)	$\mathbf{E_{corr}}$V(SCE)	$\mathbf{\eta_p}$%
	A5052		
No Inhibitor	7.32	-0.625	-
0.0003	3.28	-0.572	35.23
0.0009	2.93	-0.563	45.74
0.0020	2.55	-0.556	47.71
0.0050	2.49	-0.546	49.30
0.0070	1.54	-0.531	55.49

$\mathbf{Na_2MO_2^{-4}}$ (M)	I_{corr} ($\mu A\ cm^{-2}$)	E_{corr}V(SCE)	η_p%
	A5754		
No Inhibitor	66.95	-0.739	-
0.0003	16.60	-0.591	31.26
0.0009	15.70	-0.581	32.45
0.0020	15.50	-0.574	37.66
0.0050	13.40	-0.572	47.55

Aside from that, because of the oxidising capability of the adsorbed molybdate species, an oxidation reduction process can be initiated at flaws in the oxide-covered film, resulting in the reduction to $\mathrm{MoO_2}$ (Foad El-Sherbini et al., 2006).

$$MoO_4^{2-} + 2e^- + 4H^+ \rightarrow MoO_2 + 2H_2O \qquad (4.3)$$

The creation of this reduced form of $\mathrm{MoO_2}$ in equation 4.3 above enhance the corrosion resistance of the A5052 and A5754 alloys from the corrosive media of H_2SO_4.

This was successfully established as describe in Table by M. A. Deyab et al. (2017) that the efficacy of the sodium molybdate ($Na_2MO_2^{-4}$) inhibitor prove to protect the A5052 and A5754 from corrosion as the concentration of inhibitor increased, and also, lower the corrosion current (i_{corr}) density.

4.2.1.3 Corrosion mechanism of AA5083 containing Phosphate

Seminal contributions have been made by Wang et al. (2021) where this paper review the A5083 corrosion mechanism in seawater and seawater containing phosphate. Table 4.4 shows the chemical composition of A5083 that has been tested in this study. This literature studies of theoretical analysis limited to seawater containing phosphate, however the efficacy comparison of corrosion mechanisms in saltwater and seawater including phosphate will be revealed in the subtopic concluding section. The literature review discovered that the impacts of phosphate in the seawater were two-fold after investigated through Potentiodynamic Polarization and Scanning Electron Microscope (SEM). The electrode material utilised in the experiment was a Chinese-made 5083 aluminium alloy. The seawater was collected from the Shandong Sea. The initial pH of the corrosive medium was 7.9, and the temperature was held at 25°C with tolerance of ±0.2°C. Then, the content of phosphate was increased to $0.025\ mmol\ L^{-1}$ by adding analytical pure $Na_2HPO_4 \cdot 12H_2O$ added in to collected seawater is referred to as "seawater containing phosphate"(Wang et al., 2021). The total phosphate concentration was raised to $0.025\ mmol\ L^{-1}$. Prior to each experiment, Wang et al. (2021) performed all experiments were carried out in an airtight system at a temperature of 25°C. The potential was scanned from OCP to +300 mV versus OCP at a $1\ mVs^{-1}$ sweep rate to get Potentiodynamic Polarization curves and were performed at least three times.

In the early stages of corrosion, Wang et al. (2021) highlights that the effect of phosphate marginally increased the corrosion of 5083 in seawater. In the adsorption process on the A5083 alloy surface, hydrogen phosphate (HPO_4^{2-}) competed with hydroxide (OH^-) which weakening the interaction between OH^- and Al^{3+} near the alloy interface. This inhibited the formation of the passive film as well as its self-repair, which resulted in the activation dissolution process being accelerated.

Table 4.4: A5058 of chemical composition

Elements	Si %	Cu %	Mg%	Zn %	Mn %	Ti %	Cr%	Fe %	Ai%
A5058	0.4	0.1	5.0	0.25	1.0	0.15	0.25	0.4	92.45

The analysis conducted by Wang and his team (2021) found the evidence that the corrosion current density (i_{corr}) was greater in phosphate-containing saltwater, according to the polarisation curve. In saltwater, however, the addition of phosphate had no effect on the cluster location of the second phase of 5083, but it did change the composition of the corrosion product layer and had a clear inhibitory effect on A5083 local corrosion. Figure shows an anodic polarization curve of the AA5083 after immersed for 1 and 16 days in a seawater solution, with and without containing phosphate. The E_{pitt} of AA5083 immersed in seawater for 16 days was found to be greater than E_{pitt} of 1 day, Wang et al. (2021) suggested that the pitting resistance of the alloy surface was gradually improved as a result of the growth of the corrosion product film. The result of this analysis is then compared with the corrosion current density (i_{cor}) of seawater, with and without phosphate when soaked for the same amount of time in phosphate-containing saltwater, the i_{corr} was somewhat lower than when soaked in natural seawater, and the i_{corr} of 16 days was greater than that of 1 day, which could be explained by the decrease of surface area of the passive film and its densification (Wang et al., 2021). Table 4.5 shows the polarisation curves data that were measured. This distribution resulted in no E_{pitt} were found in A5083 soaked in seawater containing phosphate for both 1 day and 16 days.

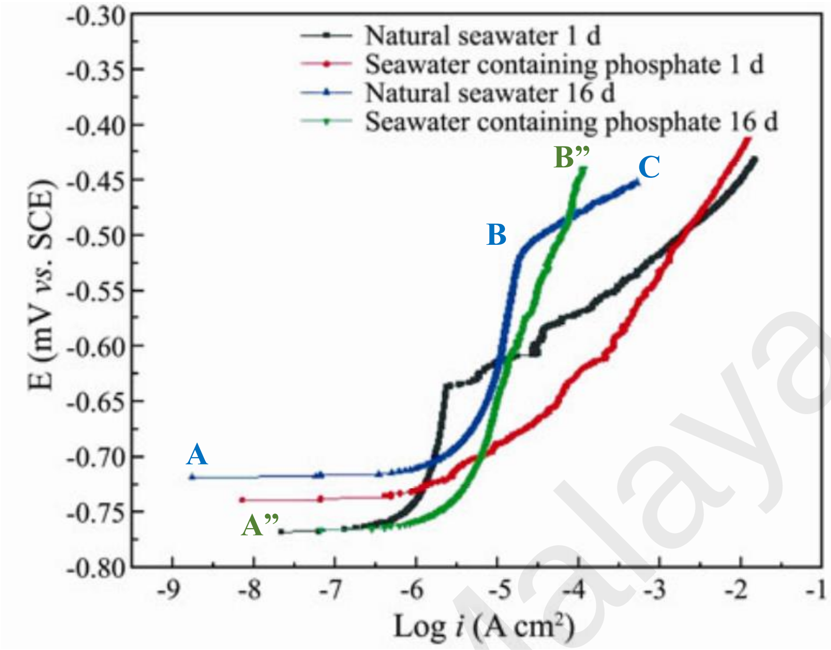

Figure 4.3: Polarization curves of AA5083 in natural seawater and seawater containing phosphate.

The polarization curve can be interpreted easily from the Figure 4.3 above. Important to note that cathodic reduction reaction is not plotted on the Figure 4.3 above thus the interpretation of polarization curves above will proceed at anodic reaction. The potential at point A (natural seawater – 16 days) and A’’ (natural seawater containing phosphate – 16days) referred to as the corrosion potential (E_{corr}) where the extrapolated anodic and cathodic Tafel slopes intersect, and the current becomes zero. On scanning in the anodic direction from point A/A”, the current density rapidly increases due to active dissolution of Al. When A progressing towards point B, the current density decreases which affirmed this phenomenon suggests the formation of passive film through a dissolution precipitation mechanism. As it reaches towards the end of the point B, the oxide concentration reaches to this maximum value. However, beyond point B, a rapid increase of current density. The curves explain the trans-passive region where the breakdown of film at a high potential. The sample experienced a breakdown, lead to formation of corrosion. On the other hand, the polarization curve for natural seawater containing phosphate also experienced the same behaviour, but there is no film breakdown occurred which the E_{pitt} (Table 4.5) were recorded. It demonstrates that the passive layer is constantly forming and shielding the alloy surface.

Table 4.5: Measurement data of polarization curves of AA5083 in two different media.

Medium	Time (d)	i_{corr} ($\mu A\ cm^{-2}$)	E_{corr} (V)	E_{pitt} (V)
Natural Seawater	1	1.23	-0.776	-0.635
	16	2.29	-0.721	-0.509
Seawater + Phosphate	1	1.29	-0.740	-
	16	2.45	-0.768	-

In an analysis of phosphate, this literature study attempted to draw fine distinctions on the influence affecting the corrosion mechanism of A5083. Wang et al. (2021) identified that the addition of phosphate has no influence on the pH of the natural saltwater even though 90% of the phosphate group in saltwater resides as HPO_4^{2-}, with constant concentration of $0.025\ mmol\ L^{-1}$. Subsequently, the phosphate in saltwater has an inhibitory effect on pitting corrosion that is not due to the pH effect. As shown in Figure 4.4, the interpretation could be separated into three stages on the effect of phosphate in saltwater on the corrosion of 5083 aluminium alloy changed over time starting from original state until final stage.

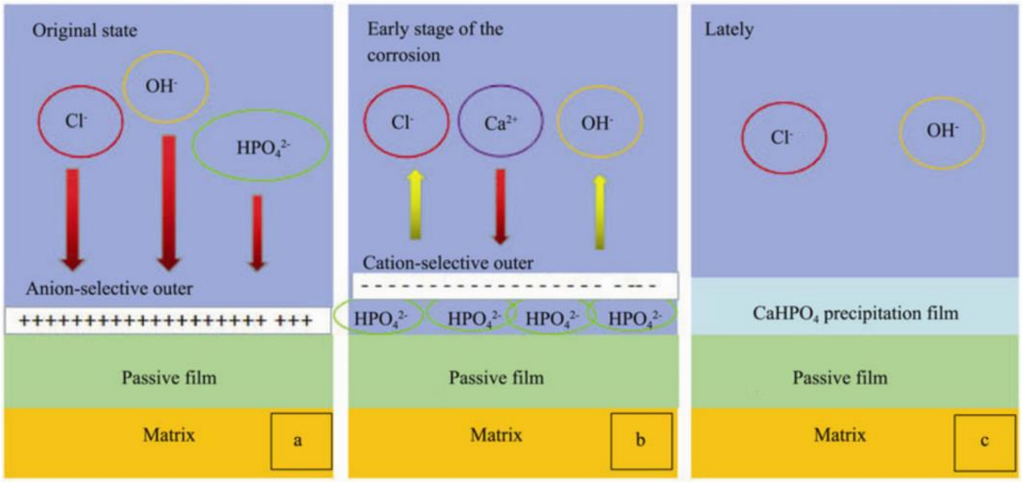

Figure 4.4: Flow process on the effect of high phosphate levels in saltwater on the corrosion of the 5083-aluminium alloy.

From the original state in Figure 4.4a above, key findings emerge behaviour and interaction between the solution and the alloy. There was an anion selective outer on the surface of the alloy in its original condition arise from the process of activation dissolution and the existence positively charged of oxygen (Jafarzadeh et al., 2007). Simultaneously, on the surface of the alloy, competitive adsorption of anions such as Hydroxide (OH^{-}), Chloride (Cl^{-}), and Hydrogen Phosphate (HPO_4^{2-}) took place. Then, the adsorption and incorporation of HPO_4^{2-} resulted in the change of the anion-selective outer passive film of A5083 into cation-selective phases in the early stages of corrosion in Figure 4.4b, according to the adsorption model described by Sato (1989) is based on the so-called bipolar passive film. The adsorption of Chloride (Cl^{-}) and Hydroxide (OH^{-}) hindered by repulsive interaction of cation selective phases which helped to inhibit the pitting corrosion. Contrarily, self-passivation process of the a5083 alloy was also inhibited. Important to note that Basame & White (2000) in his literature theorizing that Anions would contaminate the passive film components if they were present, which could explain why the corrosion rate of A5083 in saltwater with addition of phosphate was slightly higher than in natural seawater during the early stages of corrosion which the whole process broadly in line with autocatalytic acceleration. In the final process depicted in Figure 4.4c, the formation of $CaHPO_4$ on the surface of the alloy was formed under the combination of Calcium (Ca^{2+}) and Hydrogen Phosphate (HPO_4^{2-}). As the precipitation accumulated, a dense precipitation film formed, which covered the alloy's surface and served as a barrier and protection.

$$Ca^{2+} + HPO_4{}^{2-} \rightarrow CaHPO_4 \qquad (4.4)$$

Wang et al. (2021) speculated that the corrosion resistance of the alloy in seawater containing phosphate will steadily improve as the precipitation film becomes more uniform. These findings provide a valuable mechanism where the study deduced a conclusion that high concentration of phosphate confirmed to reduce the pitting tendency of A5083, inhibiting the adsorption of corrosive ions. However, high concentrations of Phosphate in seawater did not impair with self-passivation during the early stages of corrosion, thus, high concentration of phosphate in saltwater were shown to be detrimental. At this stage of understanding, it is believed that the film will offer better protection as the barrier film gradually improved with the passage of corrosion time as well as concentration(Wang et al., 2021).

4.2.1.4 Corrosion mechanism of AA5052 containing nitrate with synergism effect

The findings on efficacy of inorganic inhibitors in the previous literature at least hint that the efficiency of the inhibitors to prevent corrosion on the alloy improved as the concentration increased. However, certain inorganic inhibitor has its limitation on concentration which will need to collaborate with other inhibitor to breaks its limitation and enhance more towards the protection of alloy surface. This collaboration called synergistic inhibition effect. The findings and contribution produced by single inhibitors and the synergistic inhibition effect are studied by Liu et al. (2016) and Zhu et al. (2019). The inhibitor employed in both studies is cerium nitrate, however, inhibitor used for synergism effect is different. Nevertheless, the alloy utilised in both studies also are the same as stated in Table 4.6. A recent study by Zhu et al. (2019) investigated the synergistic effect of cerium (III) ions and glutamic acid (Glu) on corrosion inhibitions for AA5052 in sodium chloride solution. Similarly, Liu et al. (2016) also conducted the same research but using sodium dodecylbenzenesulfonate (DBS) instead of glutamic acid. In summary, both investigations also looked into the effect of a single inhibitor on the AA5052 alloy before compared the result of synergistic inhibition effect. The parameters for both studies were the same. Therefore, this section will present a review on the efficacy of nitrate as an inhibitor in protecting the alloy from corrosion based on its concentration, limitation, and synergism effect with another inhibitor.

Table 4.6: Chemical composition of AA5052 alloy. (Liu et al., 2016; Zhu et al., 2019)

Elements	Al %	Mg %	Fe %	Cr %	Zn %	Cu %	Mn %	Si %
A5052	96.76	2.46	0.27	0.19	0.10	0.10	0.06	0.06

To start with a literature studied by Zhu and his team (2019), the AA5052 alloy were immersed in a corrosion medium of sodium chloride ($NaCl$) with concentration at 3 wt%. Analytical grade reagents cerium nitrate ($Ce(NO)_3H_2O$) and glutamic acid (Glu) were used as an inhibitor. The electrochemical experiment was conducted at a temperature of 25℃ with scan rate of 1 mV/min, ranging from -300 to +300 mV. Following Table lists the electrochemical data of corrosion potential (E_{corr}), corrosion current density (i_{corr}), and inhibition efficiency (IE%) with different concentration for glutamic acid (Glu), cerium nitrate (Ce^{3+}) and Glu with addition of Ce^{3+}.

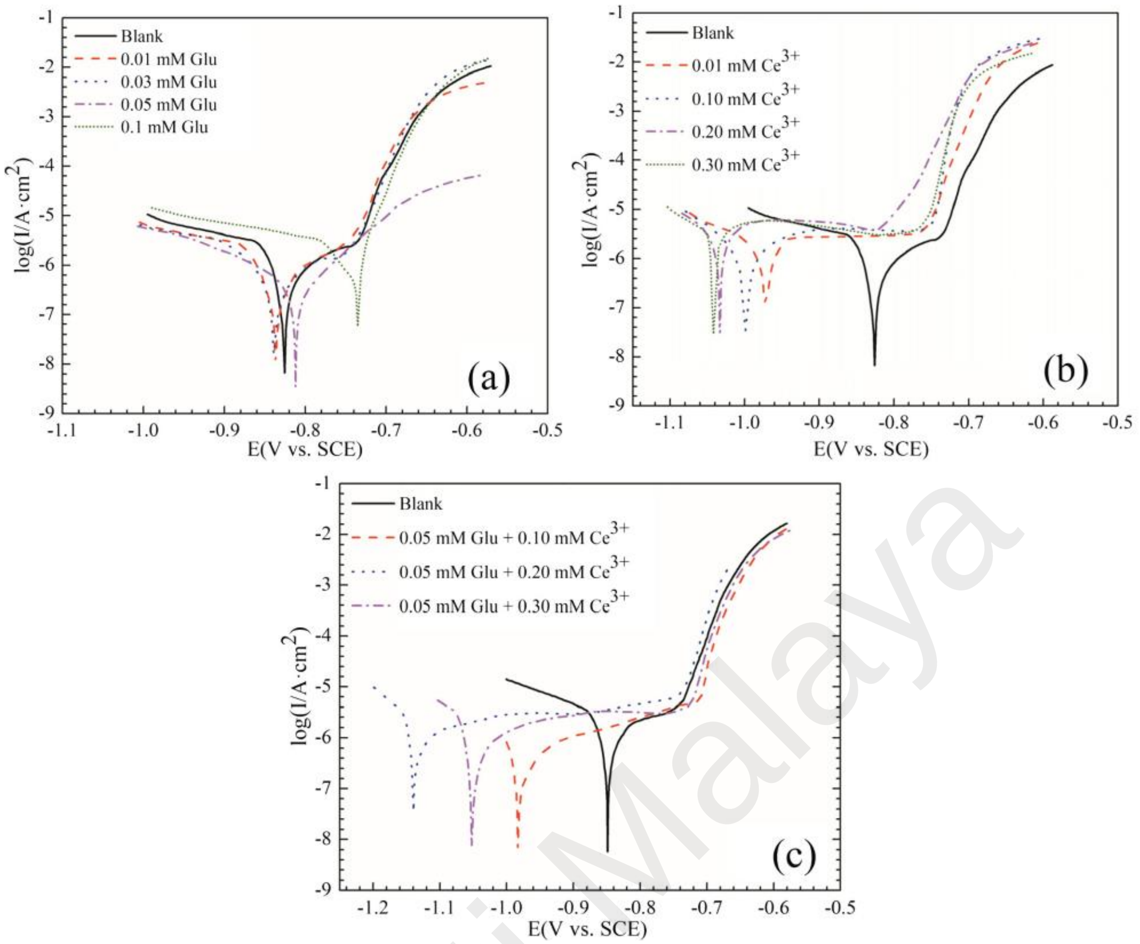

Figure 4.5: Result of polarization test on AA5052 alloy immersed in 3 wt% NaCl solution with different inhibitors on each test (a) glutamic acid, (b) cerium nitrate, and (c) glutamic with cerium nitrate. (Zhu et al., 2019)

The anodic and cathodic polarisation curves of AA5052 aluminium alloy immersed in 3 wt% NaCl solution with and without inhibitor are shown in Figure 4.5. The chemical reaction of AA5052 exposed to sodium chloride (NaCl) are shown below as cathodic reduction (Liu et al., 2016; D. Q. Zhang et al., 2012) where leads to rises in the local pH.

$$O_2 + 2H_2O + 4e^- \rightarrow 4OH^- \qquad (4.5)$$

This reaction above devotes to the dissolution of AA5052 and easily forming an oxide coating on the surface of the alloy. The chemical reaction can be easily converted as shown below:

$$Al + 3OH^- \rightarrow Al(OH) + 3e^- \qquad (4.6)$$

Chloride ions, on the other hand, are thought to adsorb on the oxide surface and speed up the reaction by producing a dissolved oxychloride complex. Over time, the passive layer will break down, and pitting corrosion will begin to take place. Thus, reaction of alloy with chloride led to the formation of chemical reaction as shown:

$$Al^{3+} + 4Cl^{-} \rightarrow AlCl_4^{-} \tag{4.7}$$

$$Al^{3+} + 2Cl^{-} + 2OH^{-} \rightarrow Al(OH)_2Cl_2^{-} \tag{4.8}$$

The study led to observe the polarization curve in Figure 4.5. In consideration of the polarization curve in Figure 4.5a confirmed the finding the glutamic acid (Glu) in this case works as a mixed type of corrosion inhibitor to AA5052 alloy. Zhu et al. (2019) observed that the influence of glutamic acid (Glu) has no effect on the polarization curves profile, thus, the inhibitor has no effect on the corrosion reaction mechanism and only adsorbed on the electrode surface. However, it been previously reported in the literature of Ashassi-Sorkhabi et al. (2005) and Zapata-Loría & Pech-Canul (2014) have proved that glutamic acid able to inhibit metal corrosion when Glu molecules is chemically adsorbed onto the surface material which did not impair to the investigation conducted by Zhu et al. (2019). Judging from the data provided in the Table 4.7, the inhibition effect of Glu reaches maximum at 62.96% when concentration is within 0.05 mM. The inhibition efficiency fell to 40% as the concentration increase to 0.10 mM. The concentration within 0.05 mM also proved that the corrosion current density (i_{corr}) is decreased.

Moving on to Figure 4.5b, cerium nitrate $\mathrm{Ce(NO_3)_3}$ are tested as an inhibitor with different concentration in 3 wt% of NaCl. It reveals the apparent passivation zones in anodic curves and the corrosion potential shifted to more negative values, therefore, proved the formation of protective layer on the surface of the alloy. The formation occurred due to the chemical reaction of cathodic region which explained the deposition of Ce-hydroxides and cerium oxides at the cathodic sites. When deposition applied to active areas, the layer acts as a barrier, preventing corrosion reactions from occurring (Machkova et al., 2013). In result, $\mathrm{Ce(NO_3)_3}$ alone proved to inhibit the corrosion mechanism but, only limited to not more than 0.20 mM concentration as per shown in Table 4.7.

Table 4.7: List of electrochemical polarization data of AA5052 alloy immersed in 3 wt% NaCl solution containing different inhibitors. (Zhu et al., 2019)

Inhibitors	$-Ecorr$ (V)	$-Icorr$ $(A\ cm^{-2})$	IE %
Blank	0.828	4.59×10^{-7}	-
0.01 mM Glu	0.836	2.49×10^{-7}	45.75
0.03 mM Glu	0.838	2.38×10^{-7}	48.15
0.05 mM Glu	0.812	1.70×10^{-7}	62.96
0.10 mM Glu	0.735	2.70×10^{-7}	41.18
0.01 mM $\mathrm{Ce^{3+}}$	0.95	3.18×10^{-7}	30.72
0.10 mM $\mathrm{Ce^{3+}}$	1.00	1.76×10^{-7}	61.66
0.20 mM $\mathrm{Ce^{3+}}$	1.02	1.39×10^{-7}	69.78
0.30 mM $\mathrm{Ce^{3+}}$	1.03	1.65×10^{-7}	63.60
0.05 mM Glu + 0.10 mM $\mathrm{Ce^{3+}}$	0.990	1.62×10^{-7}	64.71
0.05 mM Glu + 0.20 mM $\mathrm{Ce^{3+}}$	1.141	1.09×10^{-7}	76.25
0.05 mM Glu + 0.30 mM $\mathrm{Ce^{3+}}$	1.050	2.54×10^{-8}	94.47

As observed in Figure 4.5c, the passivity of the AA5052 alloy increases by influence of Glu in the $\mathrm{Ce(NO_3)_3}$. The corrosion current density is significantly reduced when glutamic acid and cerium nitrate are combined, demonstrating a synergistic action between the two inhibitors. Surprisingly, the profile of the polarization curve in Figure 4.5c shows a huge improvement compared to Glu and $\mathrm{Ce(NO_3)_3}$ alone. Based on the electrochemical data in Table 4.7, the Glu concentration remains the same for the whole synergistic process and the efficiency of the inhibitor increases as the concentration of the cerium nitrate increase. At 0.05 mM Glu + 0.30 mM $\mathrm{Ce(NO_3)_3}$, the inhibitory efficiency reaches 94.47% which represent the optimal inhibition efficiency in the electrochemical data. The data also display that the synergistic effect depend on the concentration of cerium nitrate to enhance the inhibition efficiency (Zhu et al., 2019).

A similar study on synergistic effect of cerium nitrate $\mathrm{Ce(NO_3)_3}$ with other inhibitor were performed by Liu et al. (2016). As mentioned earlier, sodium dodecylbenzensulfonate were used as the second inhibitor to investigate the synergistic effect and the efficacy of the inhibitor to protect the AA5052 alloy from corrosion. By using a potentiodynamic polarisation curve and scanning electron microscopy (SEM), the inhibition of cerium nitrate $\mathrm{Ce(NO_3)_3}$ and sodium dodecylbenzenesulfonate (DBS) alone and the synergistic inhibitory impact of on corrosion of AA5052 aluminium alloy in a 3 wt% NaCl solution was examined. In the course of the electrochemical test, Liu et al. (2016) proceeds the experiment in a temperature of 25°C with a scan rate of 1 mV/s from -300 mV to +300mV versus corrosion potential (E_{corr}). Thus, the electrochemical measurements were plotted and listed shown in Figure 4.6 and Table 4.8 below. Besides, Liu and his teams (2016) also conducted a weight loss test to further corroborate the existing evidence from electrochemical measurements on corrosion mechanism and inhibition effect. From Table 4.8 below, the inhibition efficiency (η_w%) were calculated from weight loss test after 6 days of immersion in 3 wt% of sodium chlorides ($NaCl$). It is easily interpreted that the inhibition efficiency of cerium nitrate $\mathrm{Ce(NO_3)_3}$ alone gradually increase as the concentration increase. The optimal inhibition efficiency (η_w%) achieved from $\mathrm{Ce(NO_3)_3}$ is 65.5% at 20 mg/L. However, sodium dodcylbenzenesulfonate (DBS) alone shows that the maximum inhibition efficiency (η_w%) only reaches at 47.5% at 3 mg/L and decline drastically at the concentration of 5 mg/L which demonstrates that DBS offers just a limited level of protection against the alloy. The inhibition efficiency ($\eta_w\%$) attained from synergistic effect reveals that percentage efficacy constant within 80% to 90% at given concentration in Table 4.8. Yet, the interaction of these agents exemplifies the highest inhibition efficiency at 89.7% of for 15 mg/L $\mathrm{Ce^{3+}}$+5 mg/L DBS. Indeed, proved that this combination has a synergistic effect on the corrosion inhibition of the AA5052 alloy, as demonstrated in weight loss study.

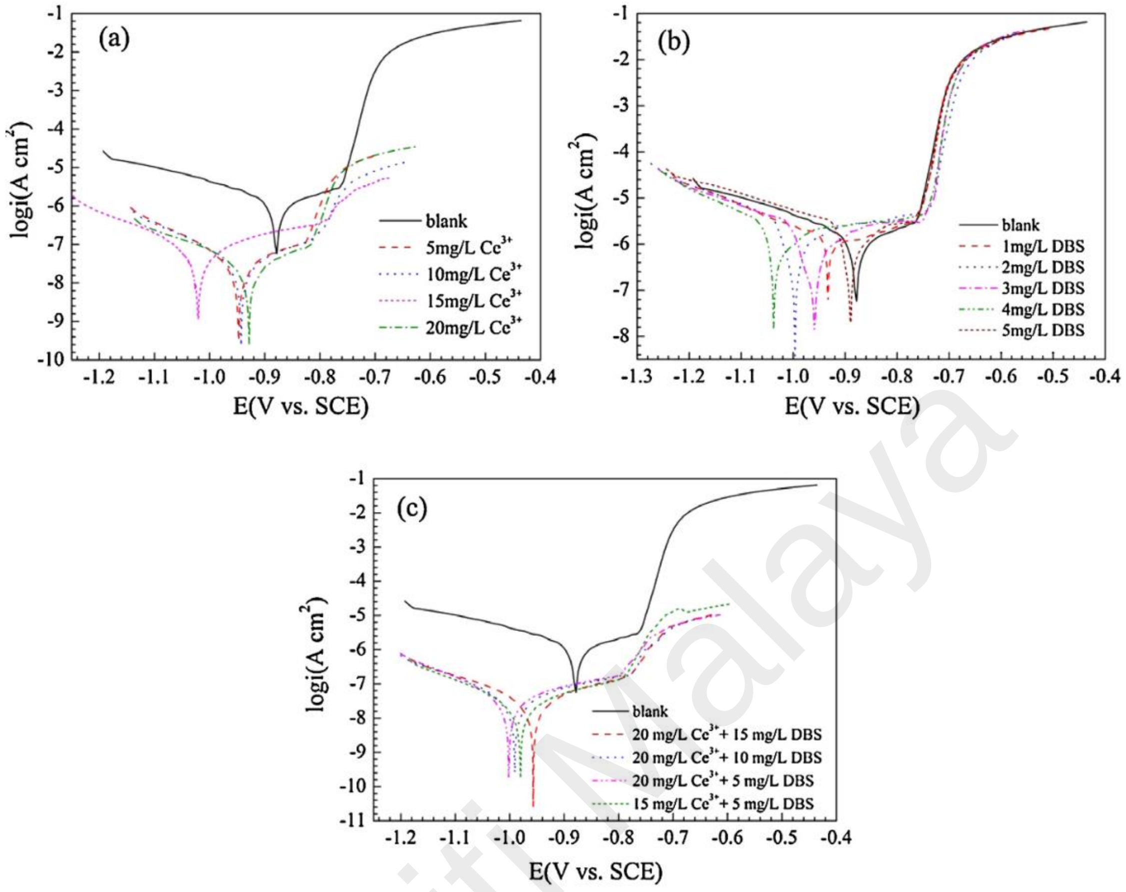

Figure 4.6: Result of polarization test on AA5052 alloy immersed in 3 wt% NaCl solution with different inhibitors on each test (a) cerium nitrate, (b) DBS, and (c) cerium nitrate with DBS. (Liu et al., 2016)

Figure 4.6 shows three different type of polarization curve of aluminium alloy 5052 immersed in 3 wt% of NaCl for 1 hour with and without inhibitor. It is generally acknowledged by Sherif (2011) in his literature that the cathodic reaction for aluminium alloy in NaCl solution is the reduction of oxygen, as shown in the following equation:

$$\frac{1}{2}O_2 + H_2O + e^- \rightarrow OH + OH^- \qquad (4.9)$$

Furthermore, when exposed to NaCl solution, aluminium alloy develops an oxide deposit on its surface as a result of the reactions that occur. Thus, aluminium dissolved into Al^{3+} due to the impact of Cl^- ions and the negative potential. Consequently, the weak spots of aluminium surface attack by Cl^- ions forming the aluminium chloride compound in the process. The reaction can be deduced as follows:

$$Al + 3OH^- \rightarrow Al(OH)_3 + 3e^- \tag{4.10}$$

$$2Al(OH)_3 \rightarrow Al_2O_3 \cdot 3H_2O \tag{4.11}$$

$$Al \rightarrow Al^{3+} + 3e^- \tag{4.12}$$

$$Al^{3+} + 4Cl^- \rightarrow AlCl_4^- \tag{4.13}$$

An overview of the polarization curve in Figure 4.6, Liu et al. (2016) justifies the formation of $\mathrm{Al_2O_3}$ causes a huge passive zone in the anodic polarisation branch of AA5052 alloy in 3wt% NaCl. Pitting corrosion of AA5052 alloy is then occurs at the potential of $-0.748\ \mathrm{V_{vs.SCE}}$ due to the dissolution of the produced oxide film resulted from the presence of high chloride ions in 3wt% NaCl. Szklarska-Smialowska (1999) in his literature of pitting corrosion on aluminium affirms that the interaction of high chloride ions to AA5052 alloy may lead to adsorption on alloy surface and subsequently form a soluble oxychloride complex ($Al(OH)_2Cl_2^-$) emanating from the reaction with $\mathrm{Al^{3+}}$ in the aluminium oxide lattice.

The second review proceeds with the presence of $\mathrm{Ce^{3+}}$ in Figure 4.6a. The outcome reveals that the corrosion potential ($\mathrm{V_{vs.SCE}}$) of AA5052 alloy offers a negative shift which agreed that the corrosion process in anodic and cathodic is retarded by the inhibition of cerium nitrate. In the work of Monticelli et al., (1991) and Shi et al. (2011) hypothesized that $\mathrm{Ce_2O_3/Ce(OH)_3}$ and $\mathrm{CeO_2/Ce(OH)_4}$ are formed from the deposition of cerium nitrate onto the surface of AA5052 alloy. The creation of layer covers the active site of the aluminium surface, obstructing electron passage and so inhibiting both the cathodic and anodic reactions. In the presence of $\mathrm{Ce^{3+}}$ ions, the passive current density reduces noticeably. Particularly, $\mathrm{Ce^{3+}}$inhibits the corrosion of AA5052 alloy in a 3wt% NaCl solution. By referring Table 4.8, the value of E_{corr} and E_{pit} shifted more towards negative as the concentration of cerium nitrate increased. The inhibition efficiency (η%) also shows that the optimal inhibition efficiency (η%) achieved at 74.4% in 20 mg/L

Ce^{3+} which the highest concentration used in this study. This validates the higher concentration will lead to better protection on the surface of the alloy. Next, Figure 4.6b shows the inhibition of DBS alone in a 3wt% NaCl solution. Liu et al. (2016) explained the behaviour of polarization curve shows that DBS hindered the cathodic process by shifting the corrosion potential in a negative direction, however, DBS has minor influence on the anodic reaction (Balbo et al., 2013). It also demonstrates that the presence of DBS shifted E_{corr} more towards negative value, except for E_{pit} only a slight change. On top of that, the influence of DBS to the anodic passivation of the AA5052 alloy is unaffected and no literature seem able to support this argument at the moment. A positive result indicating the inhibition efficiency (η%) of DBS from 1 mg/L DBS to 4 mg/L DBS where the percentage increase. Even so, when concentration of DBS at 5 mg/L, the inhibition efficiency $(\eta\%)$ decreased sharply from 71.6% to 38.8% and the E_{pit} changed to $-0.771\ \mathrm{V_{vs.SCE}}$. In the studies of Zhou et al. (2015), this declination is due to formation of micelles which retard the inhibition effect and desorption. This also confirmed that DBS prevents the formation of chloride and repairs the defects on the oxide film on the surface area by the adsorption of DBS molecules.

Table 4.8: Weight loss efficiency result and list of electrochemical polarization data of AA5052 alloy immersed in 3 wt% NaCl solution containing different inhibitors. (Liu et al., 2016)

Inhibitors	E_{corr} (V_{vsSCE})	E_{pitt} (V_{vsSCE})	η_w%	η%
Blank	-0.877	-0.748	-	-
5 mg/L Ce^{3+}	-0.947	-0.820	61.0	68.0
10 mg/L Ce^{3+}	-0.943	-0.812	63.4	75.4
15 mg/L Ce^{3+}	-1.04	-0.787	63.8	69.0
20 mg/L Ce^{3+}	-0.929	-0.825	65.5	74.4
1 mg/L DBS	-0.923	-0.760	27.6	62.4
2 mg/L DBS	-0.997	-0.751	36.4	71.9
3 mg/L DBS	-0.959	-0.749	47.6	73.9
4 mg/L DBS	-1.031	-0.750	45.5	71.6
5 mg/L DBS	-0.890	-0.771	15.7	38.8
20 mg/L Ce^{3+} + 15 mg/L DBS	-0.955	-0.781	86.2	84.4
20 mg/L Ce^{3+} + 10 mg/L DBS	-0.992	-0.768	85.4	83.3
20 mg/L Ce^{3+} + 5 mg/L DBS	-1.00	-0.772	82.6	81.6
15 mg/L Ce^{3+} + 5 mg/L DBS	-0.980	-0.801	89.7	87.8

Result in Figure 4.6c shows the polarization curves of cerium nitrate $Ce(NO_3)_3$ associate with sodium dodecylbenzensulfonate (DBS). Based on the Table 4.8, the value of E_{corr} and E_{pit} both decrease further. The corrosion reaction in both anodic and cathodic reactions are drastically inhibited. According to the findings, the inhibition efficiency (η%) of 15 mg/L cerium nitrate + 5 mg/L DBS is 87.8% which provided the best protection effect, thus, the association of $Ce(NO_3)_3$ and DBS proved to enhance more protection on the AA5052 alloy and certify the synergistic effect (Liu et al., 2016).

Summarising, cerium nitrate on both literatures showed the inhibition efficiency on the AA5052 alloy increase as the concentration increase. Despite this, the inhibition efficacy of cerium nitrate can be intensified by adding other inhibitor to provide better corrosion protection.

4.3 Surface morphology/characterization study

The surface morphology of the 5xxx series of aluminium alloy under different corrosive media with or without inhibitors are characterized generally with scanning electron microscopy (SEM), optical microscopy, etc. However, one concern about the findings in the journal reviewed concerning on corrosion and inhibition characterization by above methods in aluminium alloy was inconsistent, somehow, it is very limited. Taken as a whole, the next subsection of this characterization study will be reviewing surface morphological of the 5xxx series of aluminium alloy with or without inhibitor under corrosive media.

4.3.1 Surface morphology of Al-Mg in corrosive media

The surface of AA5052 and AA5754 alloy before and after immersed for 20 min in various concentration of H_2SO_4 in 25°C were examined. The surface morphology of AA5052 and AA5754 before the immersion test in sulfuric acid (H_2SO_4) were investigate by M. A. Deyab et al. (2017) using scanning electron microscopy (SEM).

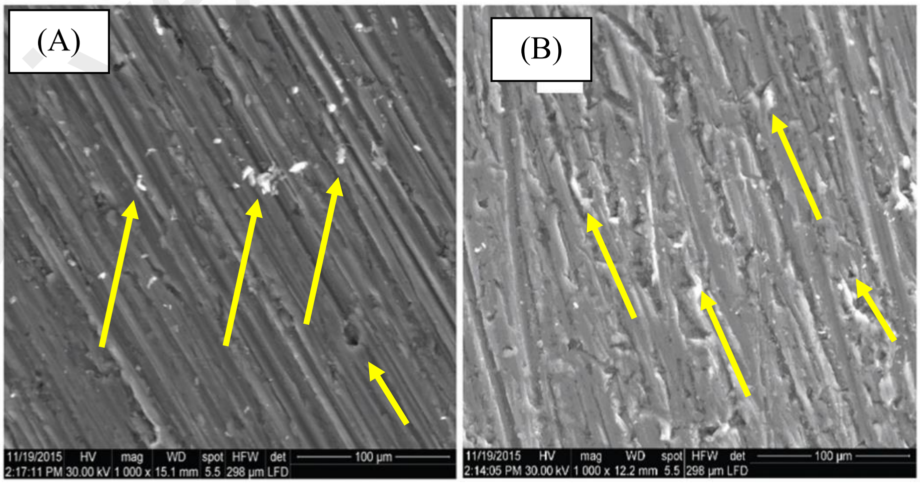

Figure 4.7: Scanning electron microscopy of (a)AA5052 and (b)AA5754 before immerse in sulfuric acid. (M. A. Deyab et al., 2017)

The surface characteristic of the aluminium alloy displays a uniform surface. However, M. A. Deyab et al. (2017) traces several inclusions such as white and dark spot present on both alloys which conclude the natural degradation of the alloys. The inclusion also known as cluster porosity (Gerrard, 2014). Experiment on AA5053 and AA5754 alloy were then immerse in 0.3M H_2SO_4 solution to study the corrosion mechanism on the surface of both alloys. In an attempt of immersion, both alloys were immersed at approximate of 20 mins before examined. The SEM photo of AA5052 and AA5754 surfaces are shown in Figure 4.8 after the immersion test completed. Evidently, the immersion in 0.3M H_2SO_4 solution resulted a rough corroded crack-like surface with significant surface damage observed on the A5052 and A5754 surfaces. M. A. Deyab et al. (2017) make no attempt in depth study of the corrosion behaviour from the findings but only to provide an adequate proof to justify the endurance of the alloy in corrosive media without inhibitor.

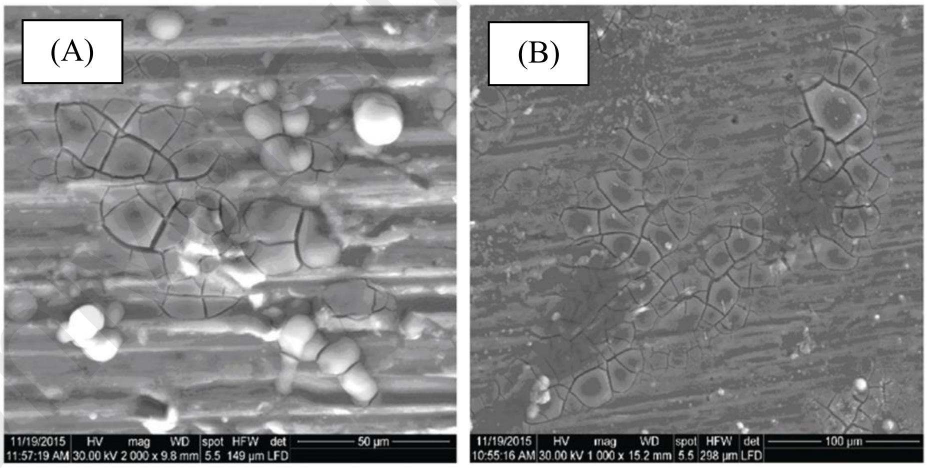

Figure 4.8: Scanning electron microscopy of (a)AA5052 and (b)AA5754 after immersed in sulfuric acid for 20 min. (M. A. Deyab et al., 2017)

A recent study, Wang et al. in 2021 also surveyed the surface characterization of aluminium alloy in corrosive media. In his study, SEM was used to examine the morphologies of corrosion of AA5083 in natural seawater for several 4 days and 16 days. In Figure 4.9a, the SEM image show the surface morphology of AA5038 after 4 days of immersion in natural seawater. It was observed that, the criss-cross like scratches on the substrate could be seen clearly. Also, the formation of corrosion product on the surface of the material had begun, but the amount produced was insufficient to cover the entire surface of AA5083 alloy. Wang et al. (2021) claims that the alloy surface homogeneity deteriorated from its initial state, and metallic inclusion in the second phase was clearly visible.

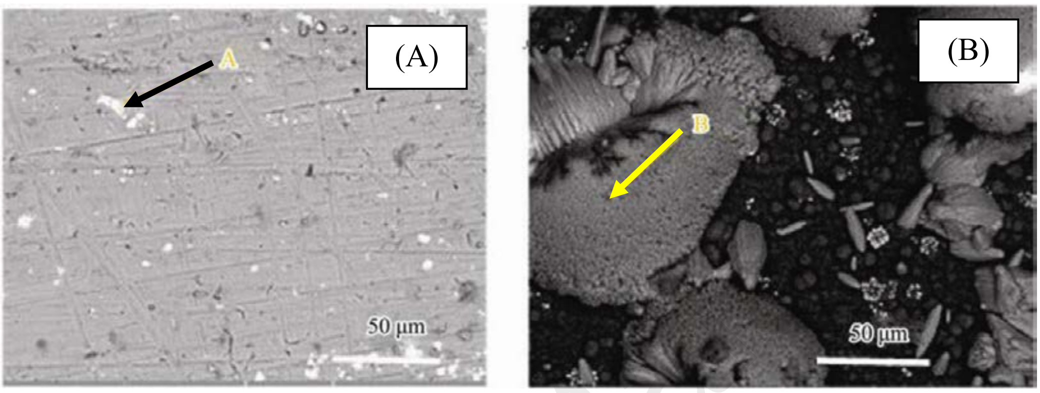

Figure 4.9: Surface morphology of AA5038 alloy in natural seawater (a)4days and (b)16days. (Wang et al., 2021)

Next in Figure 4.9b, it was observed that the corrosion product had coated the whole surface of the material after being immersed for 16 days. Thus, Wang et al. (2021) draw a distinction where formation of corrosion on AA5083 can be split into two parts where a thick layer of corrosion and other component deposited to it. In natural saltwater, CaCO3 precipitate also could be seen (Wang et al., 2021). Despite this, surface characterization of Al-Mg also attempted on sodium chlorides (NaCl) to investigate its corrosion mechanism. The study have been made by Liu et al. (2016) and Zhu et al. (2019) where AA5052 alloy immersed in 3wt% sodium chlorides (NaCl). Firstly in Liu et al. (2016) analysis, AA5052 was immersed in 3wt% NaCl for 24-hours as stated in Figure 4.10a. After 24 hours of immersion in a 3wt% NaCl solution, the surface of the AA5052 alloy was uneven and heavily suffered from corrosion. Liu et al. (2016) proposed that the spots stated ‘A’ and ‘B’ in Figure 4.10a have elemental compositions that refers to an oxidation product of aluminium. Same research were done by Zhu et al (2019), AA5052 were immersed in 3wt% NaCl, but the immersion time is 1-hour. Thus, the deterioration of the alloy observed by two analysts since the exposure time is different. From Figure 4.10b, it can be observed that the pitting corrosion exist on the surface of AA5052. The attacks of chloride ions appear to be localised, and the visible corrosion products on the surface of the AA5052 alloy matrix appear to be quite uneven.

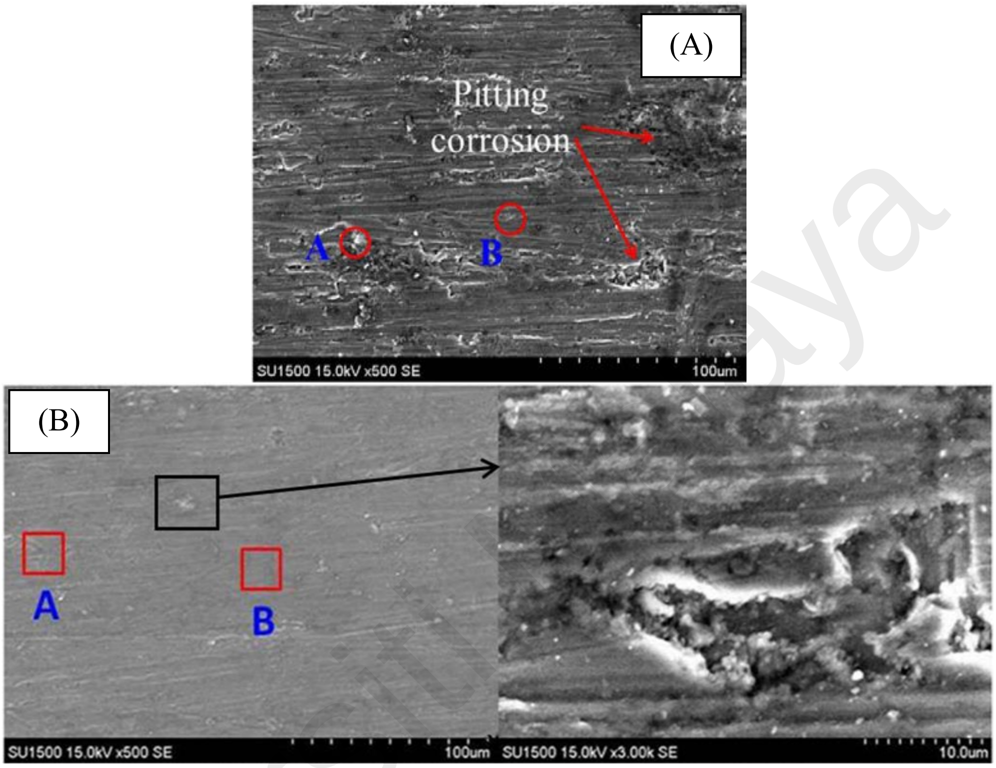

Figure 4.10: Surface morphology of AA5052 in 3 wt% sodium chlorides for (a)24-hours and (b)1-hour. (Liu et al., 2016; Zhu et al., 2019)

Generally speaking, the surface characterization on 5xxx series of aluminium alloy in different corrosive media gives a similar finding. The natural passive film generated from the alloy most likely unable to gives a better protection for a certain period of time. Hence, inhibitors are introduced to protect the surface of the material to avoid damage caused by aggressive ions. Surface morphological of the inhibited Al-Mg were also studied, thus, will be review on the next subsection.

4.3.2 Surface morphology of inhibited Al-Mg in corrosive media

The results further reviewed in line with the main objectives of this paper. According to the results reviewed in section 4.2, the electrochemical measurement proved the findings of the influence of inorganic inhibitor on the aluminium alloy gives a better protection from corrosion attack. Hence, the validity of the reviewed results reinforces with the study of surface characterization of Al-Mg alloy immersed in corrosive media with inhibitor as follows. Figure 4.11 shows a result AA5083 alloy in natural seawater containing phosphate depicted from SEM conducted by Wang et al. (2021). To begin with, SEM revealed that the surface morphology of AA5083 alloy after 4-days of immersed in seawater containing phosphate. In Figure 4.11a the corrosion attack is visible and Wang et al. (2021) concludes the morphology of the corrosion result of AA5083 alloy was identical in natural seawater shown in Figure 4.9a. However, the surface of the AA5083 alloy seems to be uniform without formation of criss-cross scratches which shows a slight improvement. Moving to Figure 4.11b, the AA5083 was immersed in natural seawater containing phosphate for 16-days. To compare, the surface morphology in Figure 4.11b contrasting the surface morphology in Figure 4.9b. Wang et al. (2021) hypothesized Ca and P were equally distributed (shown in Figure 4.11b) throughout the corrosion product, and their presence had been demonstrated in the form of dicalcium phosphate ($\mathrm{CaHPO_4}$) which gradually coated by precipitation on the alloy surface to protect from aggressive ions.

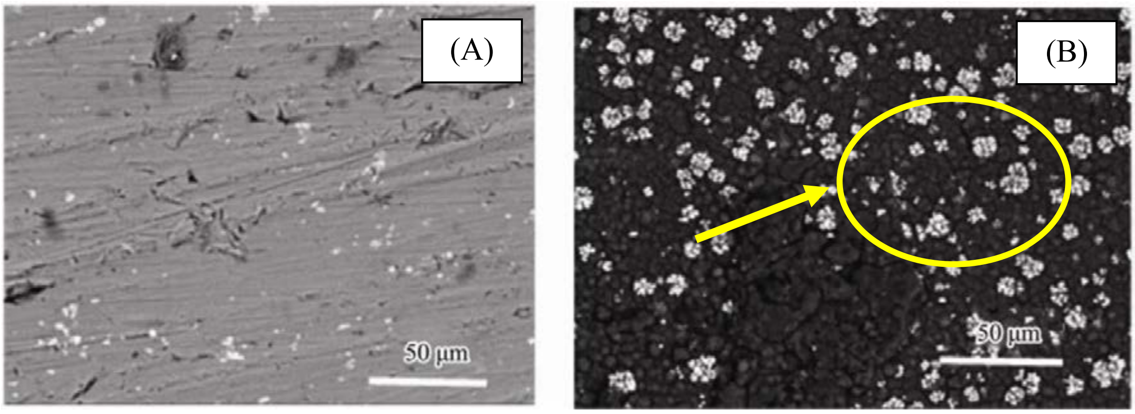

Figure 4.11: Surface morphology of AA5083 alloy in natural seawater containing phosphate (a)4days and (b)16days. (Wang et al., 2021)

The discussion is then continue with a literature by Liu et al. (2016) where he conducted the experiment on AA5052 in 3wt% sodium chlorides (NaCl) for 24-hours with different inhibitors, sodium dodecylbenzenesulfonate (DBS), cerium nitrate (Ce^{3+}), and mixture of DBS and Ce^{3+}. The result from the electrochemical measurements indicated that the cerium nitrate (Ce^{3+}), and DBS + Ce^{3+} able to protect AA5052 from corrosion. However, DBS only provide limited protection to the alloy in this case(Liu et al., 2016). Figure 4.12 shows SEM images taken from the AA5052 after immersed for 24-hours in 3wt% NaCl. A smooth uniform surface of AA5052 is shown in Figure 4.12a and Figure 4.12b with some little white particles scattered throughout. Liu et al. (2016), an authority on the literature highlights the precipitation spot discovered at “C” which underlines that DBS is adsorbed on the alloy surfaces. It implies that the DBS has a limited corrosion inhibition effect because there are only a few “C” spots on the surface of the material. It has been proposed that the "D" spot represents the surface coating of aluminium oxide. On the contrary, the presence of cerium nitrate (Ce^{3+}) on the AA5052 sample proved a significant change on the alloy surface. Interestingly, AA5052 alloy appeared to be less corroded than the sample in the solution containing only 3wt% NaCl (refer Figure 4.10a) which conclude that cerium nitrate (Ce^{3+}) gives a good protection from corrosion attack.

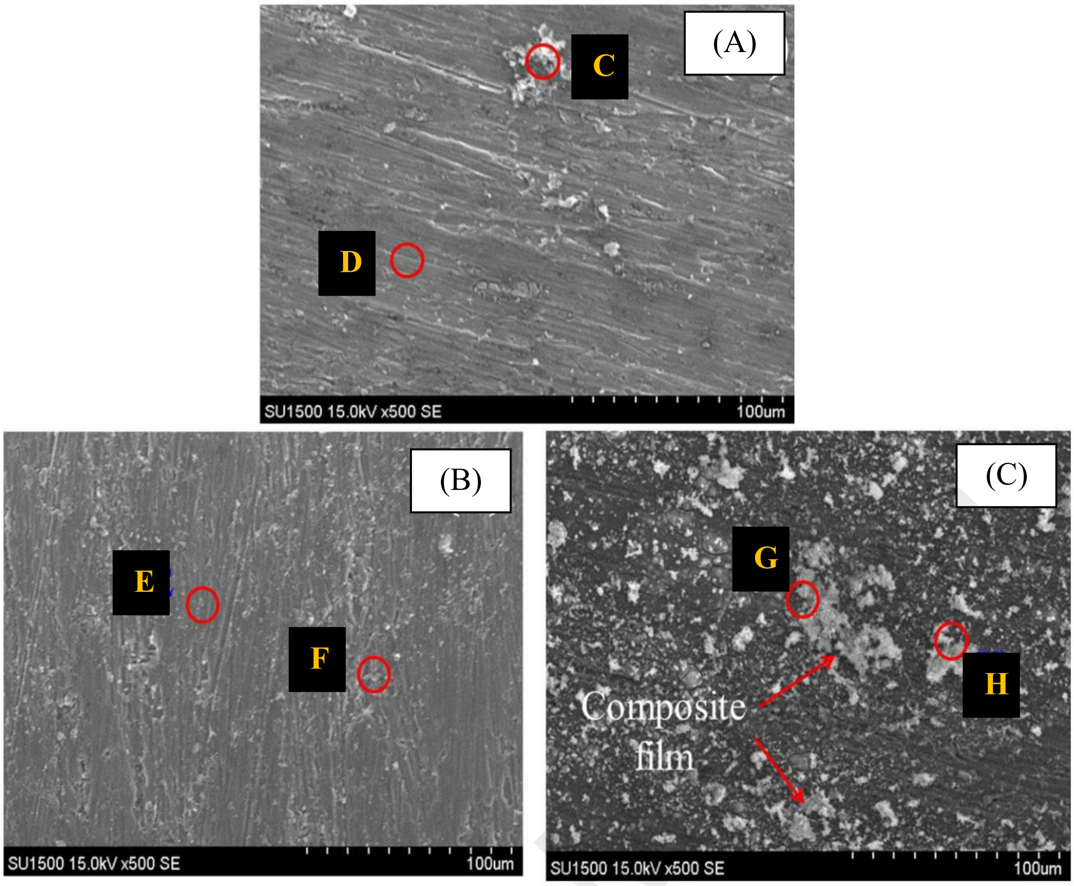

Figure 4.12: Surface morphology of AA5052 in 3 wt% sodium chlorides for 24-hours with different inhibitors (a)5 mg/L DBS, (b)15 mg/L Ce^{3+}, (c)15 mg/L Ce^{3+} + 5 mg/L DBS. (Liu et al., 2016)

In line manner with the outcome, Liu et al. (2016) points out the spots appeared on the surface of AA5052 alloy inhibited by Ce^{3+}. Again, in Figure 4.12b, the presence of Ce in the ‘E' and ‘F' spots illustrates the formation of a cerium oxide coating on the AA5052 surface. The author describes the spots also influence by the N elements due to adsorption of NO_3^- on AA5052 alloy. A remarkable compact coating forms spontaneously on the AA5052 alloy surface in the presence of a mixture of cerium nitrate and DBS inhibitors, as seen in Figure 4.12c. From the Figure 4.12c, the composite film appeared on the surface of AA5052 alloy are practically fully covered and more even. Using the ‘G' and ‘H' spots as an example, the authors suggested that the spots is owing to the formation of a complex film involving the interaction of cerium nitrate with DBS which significantly reduce the corrosion of AA5052 alloy. The spots were determined specially by using EDS spectrum to check on the element composition present in different areas.

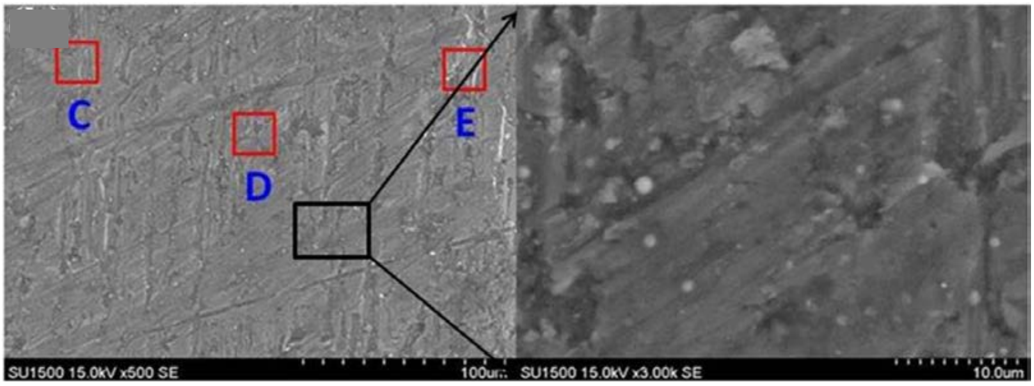

Figure 4.13: Surface morphology of AA5052 in 3 wt% sodium chlorides for 1-hour with 0.05 mM Glu + 0.30 mM Ce^{3+}inhibitor. (Zhu et al., 2019)

The same material and corrosive media used by Liu et al. (2016) were also applied in a research conducted by Zhu et al. (2019), but a slight different inhibitor used. The surface morphology of AA5052 with 0.05 mM Glu + 0.30 mM Ce^{3+} inhibitor presented in Figure 4.13. Unfortunately, the shortfall of this literature is the authors did not examine the surface morphology of the alloy with only Ce^{3+} inhibitor alone in 3wt% Nacl somewhat unable to reach a consensus on Liu et al. (2016) findings. Figure 4.13 shows the surface of the AA5052 inhibited by mixed inhibitors demonstrates a less damage caused by aggressive ions. It can be observed that the surface is relatively smoother which confirms its excellent inhibitory ability. In depth investigation were made on the surface of the AA5052 alloy (Zhu et al., 2019) from EDS spectrum data as the present carbon content in marking zones ‘C’, ‘D’ and ‘E’ slightly higher which proved the glutamic acid is present and is adsorbed on the surface of AA5052 alloy. In the zone, especially ‘C’ and ‘D’ where the present of Ce^{3+} indicates that a protective coating of cerium oxide has formed on the aluminium. The mixed inhibitor led to the development of a complex inhibitor coating on the AA5052 alloy surface (Zhu et al., 2019), thus, is credited with the corrosion inhibition. The complex film produced by the mixture of inorganic inhibitor seems to greatly improve the corrosion resistance of aluminium in the corrosive media.

CHAPTER 5: CONCLUSION & RECOMMENDATION

5.1 Conclusion

From the results and discussion of previous chapter, the following conclusion could be drawn:

i. Potentiodynamic polarization tests revealed a better corrosion resistance when 5xxx series of aluminium alloy (Al-Mg) inhibited by inorganic inhibitors.
ii. The concentration of the inorganic inhibitor proved to play vital role in protecting the Al-Mg alloy form corrosive media. As the concentration of the inorganic inhibitor increase, the inhibition efficiency will also increase as according to the tests.
iii. Influence of molybdates, chromates, nitrates, and phosphate as an inhibitor in Al-Mg alloy exhibited lower corrosion current density and lower corrosion rate resulting in a primary passivation during potentiodynamic polarization.
iv. The surface characterization of inhibited Al-Mg alloy evidenced the presence of corrosion protection layer form by inhibitor under corrosive media.

5.2 Recommendation

In this thesis research, it is recommended to conduct the experiment with variety type of inorganic inhibitor in one corrosive media at room temperature, therefore, it able to observe the inhibition efficacy and comparison under one parameter. Evaluation of the mechanical properties of corresponding Al-Mg alloys before and after inhibition is suggested for future study.

REFERENCES

Abd El Rehim, S. S., Hassan, H. H., & Amin, M. A. (2003). The corrosion inhibition study of sodium dodecyl benzene sulphonate to aluminium and its alloys in 1.0 M HCl solution. *Materials Chemistry and Physics*, *78*(2), 337–348. https://doi.org/10.1016/S0254-0584(01)00602-2

Ashassi-Sorkhabi, H., Ghasemi, Z., & Seifzadeh, D. (2005). The inhibition effect of some amino acids towards the corrosion of aluminum in 1 M HCl + 1 M H 2 SO 4 solution. *Applied Surface Science*, *249*(1–4), 408–418. https://doi.org/10.1016/j.apsusc.2004.12.016

Baboian, R., Scully, J. R., & Dean, S. W. J. (2005). Corrosion Tests and Standards. In *Corrosion Tests and Standards : Application and Interpretation*.

Balbo, A., Frignani, A., Grassi, V., & Zucchi, F. (2013). Corrosion inhibition by anionic surfactants of AA2198 Li-containing aluminium alloy in chloride solutions. *Corrosion Science*, *73*, 80–88. https://doi.org/10.1016/j.corsci.2013.03.027

Basame, S. B., & White, H. S. (2000). Pitting Corrosion of Titanium The Relationship Between Pitting Potential and Competitive Anion Adsorption at the Oxide Film/Electrolyte Interface. *Journal of The Electrochemical Society*, *147*(4), 1376. https://doi.org/10.1149/1.1393364

Bethencourt, M., Botana, F. J., Cauqui, M. A., & Marcos, M. (1997). *Protection against corrosion in marine environments of AA5083 Al–Mg alloy by lanthanide chlorides 1 ´. 250*, 455–460.

Braun, R. (1998). *Environmentally Assisted Cracking of Aluminium Alloys in Chloride Solutions* (pp. 153–164).

Brycki, B. E., Kowalczyk, I. H., Szulc, A., Kaczerewska, O., & Pakiet, M. (2018). *Organic corrosion inhibitors.* 1–32. https://doi.org/10.5772/intechopen.72943

Chaturvedi, T. P. (2009). An overview of the corrosion aspect of dental implants. *Indian Journal of Dental Research*, *20*(1), 91–98. https://doi.org/10.4103/0970-9290.49068

Choi, I. K., Cho, S. H., Kim, S. J., Jo, Y. S., & Kim, S. H. (2018). Improved corrosion resistance of 5XXX aluminum alloy by homogenization heat treatment. *Coatings*, *8*(1). https://doi.org/10.3390/coatings8010039

Constantin, F., Abrudeanu, M., & Millet, J. (2008). *CHARACTERIZATION OF CORROSION INHIBITORS BY ELECTROCHEMICAL METHODS. 3103*(19), 0–4.

Cormack, E. (2012). *The Effect of Sensitization on the Stress Corrosion Cracking of Aluminum Alloy 5456.* 1–80. http://calhoun.nps.edu/public/handle/10945/7325

Corris, R. A., Graham, M. J., Lindsay, R., Lyon, S. B., Richardson, J. A., Scantlebury, J. D., & Stott, F. H. (2013). Shreir's corrosion volume 1 Basic concepts, high temperature corrosion. In *Elsevier* (Vol. 1, Issue September 2013).

Daniel Scotto D’Antuono. (2017). *β Phase Growth and Precipitation in the 5xxx Series Aluminum Alloy System*. *May*.

Dariva, C. G., & Galio, A. F. (2016). Corrosion inhibitors: Principles, mechanisms and applications. *Corrosion Inhibitors: Principles, Mechanisms and Applications*, 1–161. https://doi.org/10.5772/57255

Davenport, A. J., Yuan, Y., Ambat, R., Connolly, B. J., Strangwood, M., Afseth, A., & Scamans, G. M. (2006). Intergranular Corrosion and Stress Corrosion Cracking of Sensitised AA5182. *Materials Science Forum*, *519–521*, 641–646. https://doi.org/10.4028/www.scientific.net/msf.519-521.641

Davis, J. R. (1999a). Aluminum and Aluminum Alloys. *Alloying: Understant the Basics*, 351–416. https://doi.org/DOI:10.1361/autb2001p351

Davis, J. R. (1999b). Corrosion of Aluminum and Aluminum Alloys. *Properties and Selection of Aluminum Alloys*, 1–262. https://doi.org/DOI: 10.1361/caaa1999p001

Deyab, M. A., El-Rehim, S. S. A., Hassan, H. H., & El-Moneim, A. A. (2017). Corrosion and Corrosion Inhibition of Aluminum Alloys A5052 and A5754 in Sulfuric Acid Solutions by Some Inorganic Inhibitors. *Zeitschrift Fur Physikalische Chemie*, *231*(6), 1141–1157. https://doi.org/10.1515/zpch-2016-0890

Deyab, M. A. M. (2015). Corrosion inhibition and adsorption behavior of sodium lauryl ether sulfate on l80 carbon steel in acetic acid solution and its synergism with ethanol. *Journal of Surfactants and Detergents*, *18*(3), 405–411. https://doi.org/10.1007/s11743-015-1671-0

Escobar, K., & Cantu, L. A. (2007). *Corrosion Basics*. *March*, 2007. http://chemwiki.ucdavis.edu/Core/Analytical_Chemistry/Electrochemistry/Case_Studies/Corrosion/Corrosion_Basics

Fan, L., Ma, J., Zou, C., Gao, J., Wang, H., Sun, J., Guan, Q., Wang, J., Tang, B., Li, J., & Wang, W. Y. (2020). Revealing foundations of the intergranular corrosion of 5XXX and 6XXX Al alloys. *Materials Letters*, *271*, 127767. https://doi.org/10.1016/j.matlet.2020.127767

Flinn Scientific. (2011). BASIC CONCEPTS OF PREPARING SOLUTIONS - Laboratory Solution Preparation. In *Safety Reference*.

Foad El-Sherbini, E. E., Abd-El-Wahab, S. M., Amin, M. A., & Deyab, M. A. (2006). Electrochemical behavior of tin in sodium borate solutions and the effect of halide ions and some inorganic inhibitors. *Corrosion Science*, *48*(8), 1885–1898. https://doi.org/10.1016/j.corsci.2005.08.002

Frankel, G. S., & McCreery, R. L. (2001). Inhibition of Al Alloy Corrosion by Chromates. *Electrochemical Society Interface*, *10*(1–4), 34–38. https://doi.org/10.1149/2.f06014if

Gerrard, A. J. (2014). *Inclusions and Hydrogen and Their Effects on the Quality of Direct Chill Cast and Flat Rolled Aluminium Alloys for Aerospace Applications By*. *September*.

Godínez, L. A., Meas, Y., Ortega-Borges, R., & Corona, A. (2003). Corrosion inhibitors. *Revista de Metalurgia (Madrid)*, *39*(2), 140–158. https://doi.org/10.3989/revmetalm.2003.v39.i2.325

Golumbfskie, W. J., Tran, K. T., Noland, J. M., Park, R., Stiles, D. J., Grogan, G., & Wong, C. (2016). Survey of detection, mitigation, and repair technologies to address problems caused by sensitization of Al-Mg alloys on navy ships. *Corrosion*, *72*(2), 314–328. https://doi.org/10.5006/1916

Hamana, D., Baziz, L., & Bouchear, M. (2004). Kinetics and mechanism of formation and transformation of metastable β′-phase in Al-Mg alloys. *Materials Chemistry and Physics*, *84*(1), 112–119. https://doi.org/10.1016/j.matchemphys.2003.11.001

Handbook, S. (2015). Corrosion and Scale Inhibitors. In *The Corrosion and Scale Handbook*. https://doi.org/10.1016/B978-0-12-803734-8.00006-0

Hayyan, M., Sameh, S. A., Hayyan, A., & AlNashef, I. M. (2012). Utilizing of sodium nitrite as inhibitor for protection of carbon steel in salt solution. *International Journal of Electrochemical Science*, *7*(8), 6941–6950.

Hill, J. A., Markley, T., Forsyth, M., Howlett, P. C., & Hinton, B. R. W. (2011). Corrosion inhibition of 7000 series aluminium alloys with cerium diphenyl phosphate. *Journal of Alloys and Compounds*, *509*(5), 1683–1690. https://doi.org/10.1016/j.jallcom.2010.09.151

Hinds, G., & Nimmo, B. (2015). *Beginners Guide to Corrosion*. *March*, 1–10.

ISO, N. S. (2015). Corrosion of metals and alloys - basic terms and definitions. *Iso*.

Ivušić, F., Lahodny-šarc, O., & Stojanović, I. (2000). *Corrosion inhibition of carbon steel by Roselle extract.pdf*. *3651*, 107–114.

Jafarzadeh, K., Shahrabi, T., Hadavi, S. M. M., & Hosseini, M. G. (2007). Role of chloride ion and dissolved oxygen in electrochemical corrosion of AA5083-H321 aluminum-magnesium alloy in NaCl solutions under flow conditions. *Journal of Materials Science and Technology*, *23*(5), 623–628.

John E. Hatch. (1984). Aluminium: Properties and Physical Metallurgy. *Science*, 1–397. https://doi.org/10.1126/science.462180

Jones, L. W. (1989). Corrosion and water technology for petroleum producers. In *Journal of Petroleum Science and Engineering* (Vol. 3, Issue 3, p. 283). https://doi.org/10.1016/0920-4105(89)90024-7

K.Sankaran, K., & S.Mishra, R. (2017). Chapter-4_Aluminium alloys_RS Mishra. In *Metallurgy and Design of Alloys with Hierarchical Microstructures*. https://doi.org/10.1016/B978-0-12-812068-2.00004-7

Kaufman, J. G. (2000). Introduction to Aluminium Alloys and Tempers. In *ASM International*.

Kausalya, T., & Hazlina, H. (2020). *Review on Corrosion Inhibitors for Oil and Gas Corrosion Issues*.

Lathabai, S., & Lloyd, P. G. (2002). The effect of scandium on the microstructure, mechanical properties and weldability of a cast Al-Mg alloy. *Acta Materialia*, *50*(17), 4275–4292. https://doi.org/10.1016/S1359-6454(02)00259-8

Liu, J., Wang, D., Gao, L., & Zhang, D. (2016). Synergism between cerium nitrate and sodium dodecylbenzenesulfonate on corrosion of AA5052 aluminium alloy in 3 wt.% NaCl solution. *Applied Surface Science*, *389*, 369–377. https://doi.org/10.1016/j.apsusc.2016.07.107

Lopez-Garrity, O., & Frankel, G. S. (2014). Corrosion Inhibition of Aluminum Alloy 2024-T3 by Sodium Molybdate. *Journal of The Electrochemical Society*, *161*(3), C95–C106. https://doi.org/10.1149/2.044403jes

Machkova, M., Matter, E. A., Kozhukharov, S., & Kozhukharov, V. (2013). Effect of the anionic part of various Ce(III) salts on the corrosion inhibition efficiency of AA2024 aluminium alloy. *Corrosion Science*, *69*(3), 396–405. https://doi.org/10.1016/j.corsci.2013.01.008

Markley, T. A., Mardel, J. I., Hughes, A. E., Hinton, B. R. W., Glenn, A. M., & Forsyth, M. (2011). Chromate replacement in coatings for corrosion protection of aerospace aluminium alloys. *Materials and Corrosion*, *62*(9), 836–840. https://doi.org/10.1002/maco.200905597

Matter, E. A., Kozhukharov, S., MacHkova, M., & Kozhukharov, V. (2013). Electrochemical studies on the corrosion inhibition of AA2024 aluminium alloy by rare earth ammonium nitrates in 3.5% NaCl solutions. *Materials and Corrosion*, *64*(5), 408–414. https://doi.org/10.1002/maco.201106349

Mazurkieicz, B. (1983). The Electrochemical Behaviour of the Al8Mg5 Intermetallic Compound. *Corrosion Science*, *23*(7), 687–690. https://doi.org/10.1002/recl.19240430102

Monticelli, C. (2018). Corrosion inhibitors. In *Encyclopedia of Interfacial Chemistry: Surface Science and Electrochemistry*. Elsevier. https://doi.org/10.1016/B978-0-12-409547-2.13443-2

Monticelli, C., Brunoro, G., Frignani, A., & Borsari, V. L. (1991). *SURFACE-ACTIVE SUBSTANCES AS INHIBITORS OF LOCALIZED CORROSION OF THE ALUMINIUM ALLOY AA 6351*. *32*(7).

Moutarlier, V., Gigandet, M. P., Pagetti, J., & Ricq, L. (2003). Molybdate/sulfuric acid anodising of 2024-aluminium alloy: Influence of inhibitor concentration on film growth and on corrosion resistance. *Surface and Coatings Technology*, *173*(1), 87–95. https://doi.org/10.1016/S0257-8972(03)00511-5

Nebti, S., Hamana, D., & Cizeron, G. (1995). Calorimetric study of pre-precipitation and precipitation in Al-Mg alloy. *Acta Metallurgica Et Materialia*, *43*(9), 3583–3588. https://doi.org/10.1016/0956-7151(95)00023-O

Nik, W. B. W., Sulaiman, O., Fadhli, A., & Rosliza, R. (2010). *CORROSION BEHAVIOUR OF ALUMINUM ALLOY IN SEAWATER*. *December*, 175–180.

Okamoto, H. (1998). Al-Mg (Aluminium-Magnesium). *Journal of Phase Equilibria*, *19*(6).

Poznak, A., Freiberg, D., & Sanders, P. (2018). Automotive Wrought Aluminium Alloys. In *Fundamentals of Aluminium Metallurgy*. Elsevier Ltd. https://doi.org/10.1016/b978-0-08-102063-0.00010-2

Roberge, P. R. (2000). Handbook of corrosion engineering. In *Choice Reviews Online* (Vol. 37, Issue 09). https://doi.org/10.5860/choice.37-5122

Rodič, P., Milošev, I., Lekka, M., Andreatta, F., & Fedrizzi, L. (2019). Study of the synergistic effect of cerium acetate and sodium sulphate on the corrosion inhibition of AA2024-T3. *Electrochimica Acta*, *308*, 337–349. https://doi.org/10.1016/j.electacta.2019.04.042

Ryen, Ø., Nijs, O., Sjölander, E., Holmedal, B., Ekström, H. E., & Nes, E. (2006). Strengthening mechanisms in solid solution aluminum alloys. *Metallurgical and Materials Transactions A: Physical Metallurgy and Materials Science*, *37*(6), 1999–2006. https://doi.org/10.1007/s11661-006-0142-7

Sanders, R. E. (2012). Aluminum and Aluminum Alloys. *Kirk-Othmer Encyclopedia of Chemical Technology*. https://doi.org/10.1002/0471238961.0112211319200112.a01.pub3

Sato, N. (1989). Toward a more fundamental understanding of corrosion processes. *Corrosion*, *45*(5), 354–368. https://doi.org/10.5006/1.3582030

Searles, J. L., Gouma, P. I., & Buchheit, R. G. (2002). Stress corrosion cracking of sensitized AA5083 (Al-4.5Mg-1.0Mn). *Materials Science Forum*, *396–402*(3), 1437–1442. https://doi.org/10.4028/www.scientific.net/msf.396-402.1437

Sehgal, A., Frankel, G. S., Zoofan, B., & Rokhlin, S. (2000). Pit Growth Study in Al Alloys by the Foil Penetration Technique. *Journal of The Electrochemical Society*, *147*(1), 140. https://doi.org/10.1149/1.1393167

Sherif, E. S. M. (2011). Corrosion and corrosion inhibition of aluminum in arabian gulf seawater and sodium chloride solutions by 3-amino-5-mercapto-1,2,4-triazole. *International Journal of Electrochemical Science*, *6*(5), 1479–1492.

Shi, H., Han, E. H., & Liu, F. (2011). Corrosion protection of aluminium alloy 2024-T3 in 0.05M NaCl by cerium cinnamate. *Corrosion Science*, *53*(7), 2374–2384. https://doi.org/10.1016/j.corsci.2011.03.012

Smallman, R. E., & Ngan, A. H. W. (2013). Modern Physical Metallurgy: Eighth Edition. In *Modern Physical Metallurgy: Eighth Edition*. https://doi.org/10.1016/C2011-0-05565-5

Starink, M. J., & Zahra, A. M. (1998). β′ and β precipitation in AN Al-Mg alloy studied by DSC and TEM. *Acta Materialia*, *46*(10), 3381–3397. https://doi.org/10.1016/S1359-6454(98)00053-6

Stojanovic, B., Bukvic, M., & Epler, I. (2018). Application of aluminum and aluminum alloys in engineering. *Applied Engineering Letters*, *3*(2), 52–62. https://doi.org/10.18485/aeletters.2018.3.2.2

Sukiman, N. L., Zhou, X., Birbilis, N., Hughes, A. E., Mol, J. M. C., Garcia, S. J., Zhou, X., & Thompson, G. E. (2013). Durability and Corrosion of Aluminium and Its Alloy: Overview, Property Space, Techniques and Developments. *Intech*, *32*(July), 137–144. http://www.intechopen.com/books/trends-in-telecommunications-technologies/gps-total-electron-content-tec- prediction-at-ionosphere-layer-over-the-equatorial-region%0AInTec%0Ahttp://www.asociatiamhc.ro/wp-content/uploads/2013/11/Guide-to-Hydropower.pdf

Szklarska-Smialowska, Z. (1999). Pitting corrosion of aluminum. *Corrosion Science*, *41*(9), 1743–1767. https://doi.org/10.1016/S0010-938X(99)00012-8

Tiu, B. D. B., & Advincula, R. C. (2015). Polymeric corrosion inhibitors for the oil and gas industry: Design principles and mechanism. *Reactive and Functional Polymers*, *95*, 25–45. https://doi.org/10.1016/j.reactfunctpolym.2015.08.006

Uma, K., Rajapriya, V., & Rekha, S. (2016). *The Effect of Inhibitor on the Corrosion of Aluminium in Acidic Solutions*. *1*, 2–7.

Umoren, S. A., Obot, I. B., Madhankumar, A., & Gasem, Z. M. (2015). Performance evaluation of pectin as ecofriendly corrosion inhibitor for X60 pipeline steel in acid medium: Experimental and theoretical approaches. *Carbohydrate Polymers*, *124*, 280–291. https://doi.org/10.1016/j.carbpol.2015.02.036

Unocic, K. a, Mills, M. J., Buchheit, R. G., & Partridge, M. (2008). Structure-Composition-Property Relationships in 5Xxx Series Aluminum Alloys. *Microscopy*.

Vargel, C., Germain, J., & Dunlop, H. (2020). *Corrosion of Aluminium Second Edition*.

Wang, J., Yang, H., Du, M., Hou, J., Peng, W., & Lin, C. (2021). Corrosion Mechanism of 5083 Aluminum Alloy in Seawater Containing Phosphate. *Journal of Ocean University of China*, *20*(2), 372–382. https://doi.org/10.1007/s11802-021-4545-2

Yakun Zhu. (2013). *CHARACTERIZATION OF BETA PHASE GROWTH AND EXPERIMENTAL VALIDATION OF LONG TERM THERMAL EXPOSURE SENSITIZATION OF AA5XXX ALLOYS*.

Yassar, R. S., Field, D. P., & Weiland, H. (2005). The effect of predeformation on the β″ and β′ precipitates and the role of Q′ phase in an Al-Mg-Si alloy; AA6022. *Scripta Materialia*, *53*(3), 299–303. https://doi.org/10.1016/j.scriptamat.2005.04.013

Yi, G., Cullen, D. A., Littrell, K. C., Golumbfskie, W., Sundberg, E., & Free, M. L. (2017). Characterization of Al-Mg Alloy Aged at Low Temperatures. *Metallurgical and Materials Transactions A: Physical Metallurgy and Materials Science*, *48*(4), 2040–2050. https://doi.org/10.1007/s11661-017-3992-2

Zaki Ahmad. (2006). Corrosion Control by Inhibition. *Principles of Corrosion Engineering and Corrosion Control*, *83*(9).

Zapata-Loría, A. D., & Pech-Canul, M. A. (2014). Corrosion Inhibition of Aluminum in 0.1 M Hcl Solution By Glutamic Acid. *Chemical Engineering Communications*, *201*(7), 855–869. https://doi.org/10.1080/00986445.2013.785944

Zhang, D. Q., Jin, X., Xie, B., Goun Joo, H., Gao, L. X., & Lee, K. Y. (2012). Corrosion inhibition of ammonium molybdate for AA6061 alloy in NaCl solution and its synergistic effect with calcium gluconate. *Surface and Interface Analysis*, *44*(1), 78–83. https://doi.org/10.1002/sia.3774

Zhang, R., Knight, S. P., Holtz, R. L., Goswami, R., Davies, C. H. J., & Birbilis, N. (2016). A survey of sensitization in 5xxx series aluminum alloys. *Corrosion*, *72*(2), 144–159. https://doi.org/10.5006/1787

Zhou, B., Wang, Y., & Zuo, Y. (2015). Evolution of the corrosion process of AA 2024-T3 in an alkaline NaCl solution with sodium dodecylbenzenesulfonate and lanthanum chloride inhibitors. *Applied Surface Science*, *357*, 735–744. https://doi.org/10.1016/j.apsusc.2015.09.093

Zhu, C., Yang, H. X., Wang, Y. Z., Zhang, D. Q., Chen, Y., & Gao, L. X. (2019). Synergistic effect between glutamic acid and rare earth cerium (III) as corrosion inhibitors on AA5052 aluminum alloy in neutral chloride medium. *Ionics*, *25*(3), 1395–1406. https://doi.org/10.1007/s11581-018-2605-4